RARγ is essential for retinoic acid induced chromatin remodeling and transcriptional activation in embryonic stem cells

Vasundhra Kashyap[1,4,*], Kristian B. Laursen[1,*], Fabienne Brenet[2], Agnes J. Viale[3], Joseph M. Scandura[2] and Lorraine J. Gudas[1,2,4,‡]

[1]Department of Pharmacology, Weill Medical College of Cornell University, 1300 York Avenue, New York, NY 10065, USA
[2]Department of Medicine, Weill Medical College of Cornell University, 1300 York Avenue, New York, NY 10065, USA
[3]Genomics Core Laboratory, Memorial Sloan-Kettering Cancer Center, 1275 York Avenue, New York, NY 10021, USA
[4]Weill Graduate School of Biomedical Sciences, 1300 York Avenue, New York, NY 10065, USA

*These authors contributed equally to this work
‡Author for correspondence (ljgudas@med.cornell.edu)

Accepted 3 December 2012
Journal of Cell Science 126, 999–1008

doi: 10.1242/jcs.119701

Summary

We have utilized retinoic acid receptor γ (gamma) knockout (RARγ$^{-/-}$) embryonic stem (ES) cells as a model system to analyze RARγ mediated transcriptional regulation of stem cell differentiation. Most of the transcripts regulated by all-trans retinoic acid (RA) in ES cells are dependent upon functional RARγ signaling. Notably, many of these RA–RARγ target genes are implicated in retinoid uptake and metabolism. For instance, Lrat (lecithin:retinol acyltransferase), Stra6 (stimulated by retinoic acid 6), Crabp2 (cellular retinoic acid binding protein 2), and Cyp26a1 (cytochrome p450 26a1) transcripts are induced in wild type (WT), but not in RARγ$^{-/-}$ cells. Transcripts for the transcription factors Pbx1 (pre-B cell leukemia homeobox-1), Wt1 (Wilm's tumor gene-1), and Meis1 (myeloid ecotropic viral integration site-1) increase upon RA treatment of WT, but not RARγ$^{-/-}$ cells. In contrast, Stra8, Dleu7, Leftb, Pitx2, and Cdx1 mRNAs are induced by RA even in the absence of RARγ. Mapping of the epigenetic signature of Meis1 revealed that RA induces a rapid increase in the H3K9/K14ac epigenetic mark at the proximal promoter and at two sites downstream of the transcription start site in WT, but not in RARγ$^{-/-}$ cells. Thus, RA-associated increases in H3K9/K14ac epigenetic marks require RARγ and are associated with increased Meis1 transcript levels, whereas H3K4me3 is present at the Meis1 proximal promoter even in the absence of RARγ. In contrast, at the Lrat proximal promoter primarily the H3K4me3 mark, and not the H3K9/K14ac mark, increases in response to RA, independently of the presence of RARγ. Our data show major epigenetic changes associated with addition of the RARγ agonist RA in ES cells.

Key words: Meis1, Differentiation, Transcription, Nuclear receptor, Retinoic acid receptor, Epigenetics

Introduction

Retinoic acid receptors (RARs) belong to the family of nuclear receptors that regulates transcription. There are three RAR isotypes (RARα, RARβ, RARγ) that heterodimerize with RXRs (RXRα, RXRβ, RXRγ) and bind the cis-acting retinoic acid response elements (RAREs) to execute the biological functions of RA during embryonic development and postnatally (Clagett-Dame and Knutson, 2011; Means and Gudas, 1995; Samarut and Rochette-Egly, 2012). While single RAR mutant mice are viable and show relatively mild phenotypes, compound mutants of RARs display an array of congenital abnormalities and die shortly after birth (Mark et al., 2009).

RARγ null mice exhibit growth deficiency (Lohnes et al., 1993). Recently, RARγ was shown to be highly expressed in the growth plate, and ablation of RARγ is associated with reduced chondrocyte proliferation and decreased expression and deposition of proteoglycans (Williams et al., 2009). These findings provide some mechanistic understanding of the growth retardation phenotype observed in the RARγ null mice. RARγ regulates hindbrain and axial patterning, and its loss results in several malformations of the axial skeleton, including anteriorization of the cervical and thoracic vertebrae (Lohnes et al., 1993; Wendling et al., 2001). RARγ is required for the formation of normal alveoli and alveoli elastic fibers in the lung (McGowan et al., 2000). Genetic ablation of RARγ results in male sterility and is associated with squamous metaplasia of seminal vesicles and the prostate glands and keratinization of glandular epithelia (Lohnes et al., 1993).

Retinoids also regulate hematopoietic development, which is dependent on distinct functions mediated by RARα and RARγ (Purton, 2007). While RARα induces granulocytic differentiation, RARγ plays a critical role in maintaining the balance between the self-renewal state of HSCs and their differentiation (Purton, 2007; Purton et al., 2006). Many of the molecular targets and pathways downstream of RARγ that mediate its effects on hematopoiesis remain to be determined.

RARγ mediates the anti-proliferative and apoptotic effects of retinoids in certain tissues and cancer cells, such as melanoma and neuroblastoma cells (Meister et al., 1998; Spanjaard et al., 1997). RARγ is the principal receptor that functions in RA mediated growth arrest in keratinocytes (Goyette et al., 2000). In a model of epidermal tumorigenesis, ablation of RARγ enhanced

the tumor incidence of Ras transformed keratinocytes and was associated with resistance to retinoid mediated growth arrest and apoptosis (Chen et al., 2004).

Studies conducted in our laboratory have shown that the lack of both alleles of RARγ in F9 teratocarcinoma stem cells is associated both with impaired differentiation and greatly reduced expression of genes involved in cell differentiation, such as Hoxa1, laminin B1, and collagen IV (α1) (Boylan et al., 1993; Boylan et al., 1995). A microarray analysis of F9 RARγ null teratocarcinoma stem cells revealed novel RARγ regulated genes, reinforcing its important role in retinoid signaling and differentiation (Su and Gudas, 2008a; Su and Gudas, 2008b).

We have now utilized murine RARγ knockout ($RAR\gamma^{-/-}$) embryonic stem (ES) cells as a model system to study RARγ mediated transcriptional regulation in development and cell differentiation. ES cells are derived from the inner cell mass of blastocysts and have the unique ability to self-renew under defined conditions (Smith, 2001). ES cells have a stable genome and possess the capacity to differentiate into the three germ layers, thus making them an excellent cell culture system to study RA mediated differentiation *in vitro* (Gudas and Wagner, 2011; Soprano et al., 2007). We previously reported that RARγ null ES cells do not differentiate into parietal endoderm, an epithelial cell type, in response to RA (Kashyap et al., 2011).

To delineate further the functions of RARγ in ES cells, we performed microarray analysis of wild type (WT) and $RAR\gamma^{-/-}$ ES cells and identified differentially regulated genes. We characterized the transcriptional and epigenetic regulation of the RARγ target gene Meis1 using chromatin immunoprecipitation (ChIP) and ChIP-chip technologies. Furthermore, functional depletion of RARγ in WT ES cells, combined with restored RARγ expression in $RAR\gamma^{-/-}$ cells, confirmed the requirement for RARγ in the RA induced transcription of Meis1.

Results

Identification of differentially expressed genes in WT and RARγ knockout ES cells by microarray analysis

To identify RARγ regulated genes in ES cells, we performed microarray analyses of ES RARγ knockout ($RAR\gamma^{-/-}$) compared to wild type (WT) ES cells under different culture conditions. We cultured the WT and $RAR\gamma^{-/-}$ cells with vehicle control or 1 μM RA for 8 or 24 h. The 8 h and 24 h time points allowed us to examine the kinetics of RA induced transcript changes. The 8 h time point also provides the advantage of capturing early transcript changes that are less likely to be secondary changes related to cell differentiation.

A total of 152 transcripts were differentially regulated by threefold or more in untreated WT versus $RAR\gamma^{-/-}$ ES cells (Fig. 1). Of these 152 differentially expressed transcripts, 80 transcripts showed reduced levels (Fig. 1; supplementary material Table S2A), and 78 transcripts showed elevated levels in the $RAR\gamma^{-/-}$ cells compared to the WT cells in vehicle treated (untreated) conditions (Fig. 1; supplementary material Table S2B). These data suggest a role for RARγ in regulating gene expression in the absence of the ligand, as we demonstrated in teratocarcinoma stem cells for RARα (Laursen et al., 2012). Furthermore, a total of 56 and 72 transcripts were differentially regulated by threefold or more in WT versus $RAR\gamma^{-/-}$ ES cells upon 8 and 24 h of RA treatment, respectively (Fig. 1; supplementary material Table S3A,B, Table S4A,B).

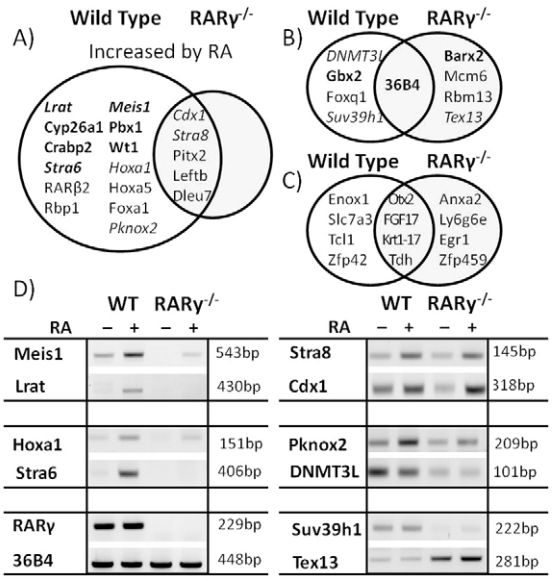

Fig. 1. Microarray analysis of transcript levels in WT and $RAR\gamma^{-/-}$ ES cells. (**A**) Genes that show elevated transcript levels upon RA treatment for 24 h. The white circle shows genes induced by RA in WT ES cells; the gray circle shows genes induced by RA in RARγ null ES cells. The $RAR\gamma^{-/-}$ ES cells were generated as described previously (Kashyap et al., 2011). The microarray data were generated from a single-cell cloned ES cell line. (**B**) Genes that are differentially expressed between untreated (vehicle only) WT and $RAR\gamma^{-/-}$ cells at 24 h. The white circles show genes expressed at a higher level in untreated WT than $RAR\gamma^{-/-}$ cells. The gray circles show genes expressed at a higher level in untreated $RAR\gamma^{-/-}$ than in WT. (**C**) Genes that show decreased transcript levels upon RA treatment for 24 h. The white circle shows genes repressed by RA in WT cells. The gray circle shows genes repressed by RA in $RAR\gamma^{-/-}$ cells. Genes validated by real time RT-PCR are shown in bold. Note that the Venn diagrams depict only a subset of the genes identified in each group (for complete lists, refer to the supplementary material Tables S2–S7). (**D**) Validation of transcript levels in WT and $RAR\gamma^{-/-}$ ES cells by end-point PCR. Meis1, Lrat, Hoxa1, Stra6, and Pknox2 display reduced RA dependent induction in $RAR\gamma^{-/-}$ cells relative to WT, whereas Stra8 and Cdx1 are induced in the absence of RARγ. DNMT3L, Suv39h1, and Tex13 are differentially expressed between WT and $RAR\gamma^{-/-}$ ES cells in an RA independent manner. Experiments in D were performed multiple times with identical results; representative samples are shown.

Transcripts are differentially regulated by RA in WT and RARγ knockout cells

To identify the genes that were regulated by RA treatment, we analyzed the fold changes in WT and $RAR\gamma^{-/-}$ ES cells independently upon 8 and 24 h of RA treatment in comparison to the untreated controls for each cell line. A total of 29 and 91 transcripts were increased 2.5-fold in WT ES cells upon 8 and 24 h of RA treatment, respectively, compared to untreated WT (Fig. 1A; supplementary material Tables S5, S6). The 2.5-fold cut-off was selected based on advice from the Weill Cornell Bioinformatics Core staff. Transcript levels of many known RA target genes increased in WT ES cells in response to RA treatment, such as genes of the Hoxa and Hoxb clusters and Cdx1, $RAR\beta_2$, and Gata6 (Fig. 1A,D; supplementary material Table S5, Table S6A). Transcript levels of 40 genes decreased upon 24 h of RA treatment in WT cells (Fig. 1C; supplementary material Table S6B, Table S7B). In accord with previous studies, transcript levels of Zfp42 (Rex1), a stem cell marker, were

reduced by 2.7-fold upon 24 h of RA treatment of WT cells (Fig. 1C; supplementary material Table S6B). Only a few genes (Otx2, FGF17, Krt1-17, and Tdh) showed reduced expression levels in both WT and RARγ$^{-/-}$ cells treated with RA for 24 h (Fig. 1C; supplementary material Table S6B, Table S7B).

In contrast, only 23 transcripts were increased by 2.5-fold or more in RARγ$^{-/-}$ ES cells upon treatment with RA for 24 h compared to untreated RARγ$^{-/-}$ (supplementary material Table S7A). The 8 h RA treatment did not induce significant (>2.5-fold) changes in the levels of any transcripts in the RARγ$^{-/-}$ ES cells compared to untreated RARγ$^{-/-}$ ES cells. A large number of transcripts that were differentially regulated by 2.5-fold or more in WT cells upon 24 h of RA treatment did not show statistically significant fold changes of 2.5-fold or more in the RARγ$^{-/-}$ ES cells (Fig. 1A; supplementary material Table S4A). Thus, RARγ is implicated in regulating this group of genes and our results also suggest that other RARs, i.e. RARα and RARβ, incompletely compensate for the loss of RARγ. However, Stra8, Dleu7, Leftb, Pitx2, and Cdx1 were induced by RA by more than 3.8-fold even in the absence of RARγ.

Gene ontology revealed that the vast majority of genes which exhibit reduced expression in RARγ$^{-/-}$ cells are homeobox genes involved in morphogenesis, axis formation, and tissue patterning (Meis1, Pknox2, Pbx1, Foxq1, Gbx2, and Hox genes). RARγ plays a key role in axis specification by RA (Bayha et al., 2009). The induction of Hoxa1, Hoxa2, Hoxb1, and Hoxb2, which are involved in rhombomere/hindbrain formation (Gavalas et al., 2003), is lost in RARγ$^{-/-}$ ES cells. Reduced levels of Anxa5, Anxa2, F2r, F2rl1, and Gap43 suggest impaired wound healing in RARγ$^{-/-}$ mice. Also, the transcript levels of several P450 cytochromes (Cyp1b1, Cyp26a1, and Cyp7b1) are reduced in RARγ$^{-/-}$ cells, pointing to abnormal metabolism. Finally, reduced expression of Col4a1, Col4a2, Ccnd2, Lama1, Pik3r1, PDGFRα, and Zyxin in RARγ$^{-/-}$ versus WT suggests that focal adhesion may be impaired in RARγ$^{-/-}$ ES cells, which could lead to increased cellular mobility and/or invasiveness.

RARγ regulates RA mediated changes in the transcript levels of genes involved in retinoid metabolism, including *Stra6*, *Cyp26a1*, *Lrat* and *Crabp2*, in ES cells

Because we previously observed alterations in the expression of several genes involved in retinol metabolism during ES differentiation (Langton and Gudas, 2008), we assessed the mRNA levels of several genes that function in the retinoid metabolism pathway by real time RT-PCR to determine if they were regulated by RARγ. RA greatly increased transcript levels of Stra6, Lrat, Crabp2, and Cyp26a1 in WT cells but not in the RARγ$^{-/-}$ cells, implicating RARγ in the regulation of retinoid metabolism (Fig. 2). Stra6 is a membrane bound receptor that binds to the serum retinol binding protein (RBP4), a carrier of retinol in the blood, and Stra6 both facilitates uptake of retinol and cell signaling via STAT5 (Berry et al., 2011; Kawaguchi et al., 2007). Mutations in Stra6 cause a wide range of defects that include anophthalmia, pulmonary agenesis, diaphragmatic hernia, pancreatic malformations, mental retardation, and congenital heart defects (Golzio et al., 2007; Pasutto et al., 2007). Lrat is an enzyme that converts intracellular retinol to retinyl esters; such esters are a storage form of retinoids in the cell (Amengual et al., 2012; Batten et al., 2004; Guo and Gudas, 1998; Liu and Gudas, 2005; O'Byrne et al., 2005; Zolfaghari and Ross, 2000). Crabp2 is involved in transporting RA from the cytoplasm into the nucleus (Noy, 2000), and Cyp26a1 metabolizes RA into polar metabolites in ES cells (Langton and Gudas, 2008; White et al., 1997). Real time PCR validation showed that the kinetics of the RA mediated increases in transcript levels of Stra6, Crabp2, and Cyp26a1 are similar (Fig. 2B–D). All three transcripts increase as early as 8 h after RA addition and show increased expression at 48 h of RA treatment in WT ES cells (Fig. 2A–E). In contrast, Stra6, Crabp2, and Cyp26a1 transcripts remained much lower in the RARγ$^{-/-}$ cells (Fig. 2A–E). Lrat mRNA levels in WT ES cells increased as early as 8 h after RA addition and reached a maximum at 24 h of RA treatment, after which Lrat mRNA levels declined (Fig. 2A, black square). Lrat transcript levels did not increase in the RARγ$^{-/-}$ cells treated with RA (Fig. 2A, open triangle). The mRNA levels of the reference gene 36B4 (Rplp0) were measured as an internal control and were unchanged with RA treatment (Fig. 2E).

The Lrat gene is epigenetically altered by RA treatment

Transcriptional induction by RA is frequently associated with increased levels of transcriptional permissive marks, such as H3K9/14ac and H3K4me3, whereas the levels of transcriptional repressive marks, such as the polycomb (PcG) deposited H3K27me3, are decreased (Gillespie and Gudas, 2007b; Kashyap and Gudas, 2010; Wu et al., 2009). RA treatment for 24 h causes a ~10-fold increase in the Lrat transcript level in WT ES cells (Fig. 2A), yet the levels of H3K9/14ac marks did not significantly increase in response to RA (Fig. 2F). The levels of the epigenetic mark H3K4me3 were similar in WT and RARγ$^{-/-}$ ES cells (Fig. 2F). We also found that the Lrat gene is associated with a repressive H3K27me3 mark in untreated WT and RARγ$^{-/-}$ ES cells. While RA treatment leads to a reduction in the H3K27me3 mark in the WT ES cells, H3K27me3 levels remain high in the RARγ$^{-/-}$ ES cells and in fact, the levels of H3K27me3 at 24 h of RA treatment are higher than those in untreated RARγ$^{-/-}$ cells (Fig. 2A). Thus, our data indicate a role for RA and RARγ in the transcriptional activation of Lrat by antagonizing PcG mediated repression. We also show that RARγ is not required for the placement of H3K4me3, an epigenetic mark generally associated with transcriptionally active chromatin (Sims and Reinberg, 2006), and that the presence of this mark is not sufficient for active transcription of Lrat in RA treated RARγ$^{-/-}$ cells.

RARγ regulates transcript levels of transcription factors

We further validated the transcript levels of several transcription factors that play key roles in different aspects of differentiation during development and are differentially expressed in the WT and RARγ$^{-/-}$ cells (Fig. 3A–E). Meis1 and Pbx1 are homeodomain transcription factors that function as cofactors of Hox proteins and regulate distinct aspects of differentiation (Chang et al., 1996; Featherstone, 2003; Shanmugam et al., 1999; Shen et al., 1996; Shen et al., 1997; Soprano et al., 2007). Dysregulated expression of these cofactors in combination with Hox proteins is observed in different types of leukemia (Eklund, 2007; Wang et al., 2006). Pbx1 is required during embryogenesis for skeletal patterning, development of adrenal glands and pancreas, urogenital differentiation, nephrogenesis, and maintenance of hematopoiesis in the liver of the developing fetus (Moens and Selleri, 2006). Meis1 disruption in mice is embryonic lethal and Meis1 deficient embryos have defects in the eye, angiogenesis, and hematopoiesis (Azcoitia et al., 2005; Hisa

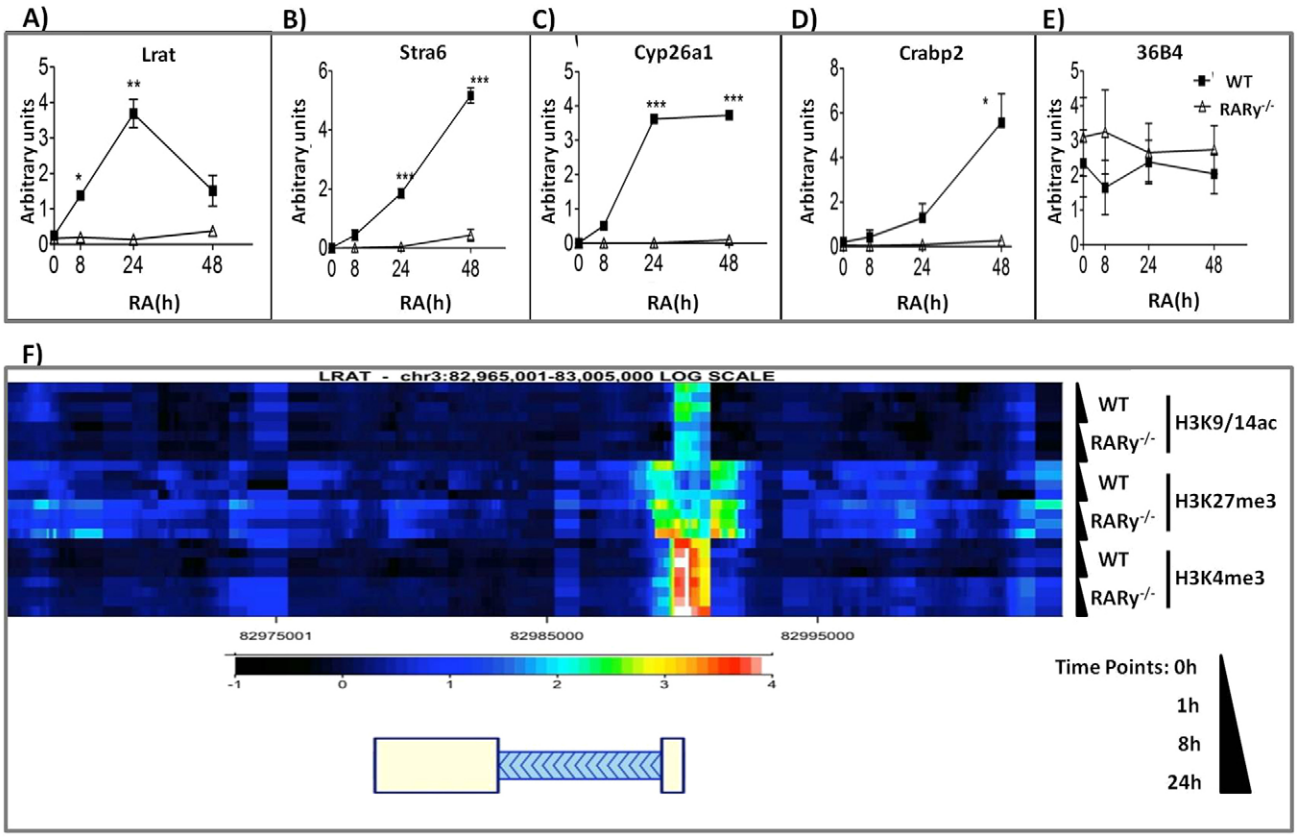

Fig. 2. RA regulated induction of retinoid metabolism genes. (**A–E**) Transcript levels of Lrat, Stra6, Cyp26a1, Crabp2, and 36B4 (a control) in WT and RARγ$^{-/-}$ ES cells. Experiments were performed three times using independent RNA samples (■ WT; △ RARγ$^{-/-}$); the error bars represent the standard error of the mean (s.e.m.). (**F**) ChIP-chip heatmap of the Lrat genomic region showing H3K9/14ac, H3K27me3, and H3K4me3 histone marks in WT and RARγ$^{-/-}$ cells upon increasing times of exposure to RA (0, 1, 8, and 24 h, black triangle). The colors represents $\log_2$-transformed ChIP enrichment in ChIP-chip data sets (replicate means). Columns show genomic loci and rows show IP condition. Statistical significance: *$P<0.05$, **$P<0.01$, ***$P<0.005$. The color scale of the $\log_2$ enrichment is indicated below the ChIP-chip data panel. The Lrat genomic location (blue tones) is indicated schematically at the bottom.

et al., 2004). Expression of Meis1 is elevated in acute myeloid leukemias, and Meis1 has oncogenic potential in leukemias that harbor fusion proteins with the translocation of MLL (mixed lineage leukemia) family members (Kawagoe et al., 1999; Wong et al., 2007). Pbx1 and Meis1 mRNA levels increase upon 24 h of RA treatment in WT cells, and transcript levels continue to increase up to 48 h of RA treatment (Fig. 3A,B). In contrast, RA did not increase Pbx1 and Meis1 transcript levels in the RARγ$^{-/-}$ cells (Fig. 3A,B).

Wt1 (Wilm's tumor gene) encodes a transcription factor that has an essential role in the normal development of the urogenital system, and is mutated in a subset of patients with Wilm's tumors, a type of kidney tumor (Kreidberg et al., 1993; Pelletier et al., 1991a; Pelletier et al., 1991b). RA increased Wt1 mRNA levels at 48 h in WT cells, but no RA dependent increase in the Wt1 mRNA levels occurred in the RARγ$^{-/-}$ cells (Fig. 3C).

Gbx2 (gastrulation brain homeobox 2) is required for normal development of mid/hindbrain region and morphogenesis of the inner ear (Lin et al., 2005; Wassarman et al., 1997). In WT cells RA treatment caused less than a twofold increase in the Gbx2 mRNA levels. Gbx2 mRNA levels were consistently lower in RARγ$^{-/-}$ cells compared to WT cells (Fig. 3D).

Barx1 is a homeodomain transcription factor that is expressed in the stomach mesenchyme and molar dental cells of mesenchymal origin (Makarenkova and Meech, 2012). Barx1 mRNA levels were 70-fold lower in untreated WT cells than in the untreated RARγ$^{-/-}$ cells (Fig. 3E). At 48 h of RA treatment Barx1 mRNA levels decreased by ~25% in the RARγ$^{-/-}$ cells, whereas Barx1 transcript levels did not change in WT cells (Fig. 3E). Thus, RA mediates changes in the transcript levels of multiple genes involved in differentiation and development that require RARγ. Why these specific genes are highly regulated by RA in differentiating WT ES cells is not yet clear.

RA induces RARγ dependent epigenomic re-organization of the Meis1 gene in WT cells

Since aberrant regulation of Meis1 is implicated in leukemia (Kawagoe et al., 1999; Wong et al., 2007) and we are interested in differentiation therapy for cancer, we next examined the dynamics of the RA induced increase in Meis1 transcript levels in further detail. We hypothesized that RA signaling would induce epigenetic changes at the Meis1 gene and that loss of RARγ would prevent such chromatin changes at this gene. In WT cells RA induced a rapid increase in H3K9/14ac levels at the proximal promoter and at specific regions (DS1 and DS2) located

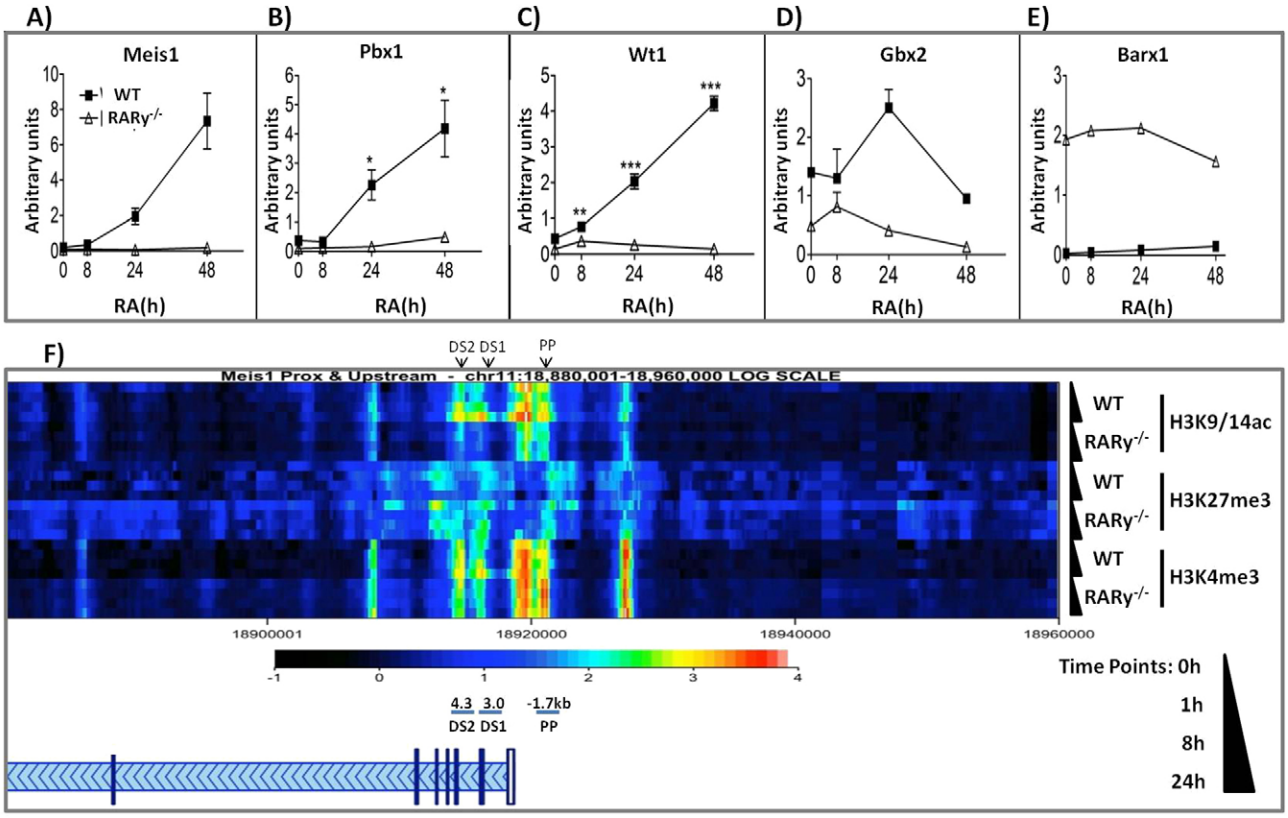

Fig. 3. RA regulated induction of transcription factors. (**A–E**) Transcript levels in WT and RARγ$^{-/-}$ ES cells of Meis1, Pbx1, Wt1, Gbx2, and Barx1. Experiments were performed three times using independent RNA samples (filled squares, WT; open triangles, RARγ$^{-/-}$); error bars indicate s.e.m. (**F**) ChIP-chip heat-map of the Meis1 proximal promoter region showing H3K9/14ac, H3K27me3, and H3K4me3 histone marks in WT and RARγ$^{-/-}$ cells upon increasing times of exposure to RA (0, 1, 8, and 24 h, black triangle). The colors represents $\log_2$-transformed ChIP enrichment in ChIP-chip data sets (replicate means). DS1 and DS2 indicate downstream sites 1 and 2; PP indicates the proximal promoter region. Columns show genomic loci and rows show IP condition. Statistical significance: $P<0.05$, $^{**}P<0.01$, $^{***}P<0.005$. The color scale of the $\log_2$ enrichment is indicated below the ChIP-chip data panel. The Meis1 exon (broad) and intron (narrow) locations (blue tones) are indicated schematically at the bottom.

downstream of the transcription start site (TSS) in the Meis1 gene (Fig. 3F, arrows; Fig. 4A). H3K9/14ac epigenetic marks are generally associated with transcriptionally active genes (Jenuwein and Allis, 2001). In contrast, the H3K9/14ac levels at the promoter and downstream intragenic regions of the Meis1 gene were much lower in the RARγ cells compared to the WT cells (Fig. 3F; Fig. 4A), correlating with Meis1 transcript levels in WT versus RARγ$^{-/-}$ cells (Fig. 3A). The H3K4me3 mark is elevated in a region surrounding the promoter of the Meis1 gene in both untreated and RA treated WT and RARγ$^{-/-}$ cells (Fig. 3F; Fig. 4C).

Meis1 resides in a bivalent chromatin domain, e.g. it is associated with both with the repressive H3K27me3 mark deposited by PcG proteins (Boyer et al., 2006) and with the permissive H3K4me3 mark described above. By 24 h of RA treatment there is a reduction in the H3K27me3 mark (Fig. 3F), and in the levels of Suz12 protein (Fig. 4B) at the promoter and in the gene body of Meis1 in WT cells. However, in RARγ$^{-/-}$ cells both the H3K27me3 mark and Suz12 levels remain high at 24 h of RA treatment (Fig. 3F; Fig. 4B). Thus, RA signaling via RARγ antagonizes the PcG mediated repression of the Meis1 gene, and the lack of RARγ prevents the removal of the H3K27me3 mark from the Meis1 gene (Fig. 3F).

Taken together, these data suggest that at the Meis1 gene RARγ (or its downstream targets) is required for RA induced changes in the epigenetic configuration comprising the H3K9/14ac marks. However, RARγ is not needed for the deposition of the H3K4me3 mark at the Meis1 promoter and the H3K4me3 mark does not correlate with transcription of Meis1 in RA treated RARγ$^{-/-}$ cells (Fig. 3F).

The Meis1 promoter proximal region appears devoid of functional retinoic acid response elements (RAREs)

The effects of RA are mediated through RAREs, and consequently the epigenomic structure exhibits dramatic changes in response to RA, generating hot-spots in the ChIP-chip maps. We evaluated the Meis1 proximal promoter region (defined as TSS −/+ 40 kb), and identified three sites exhibiting dramatic epigenetic changes in response to RA (Fig. 3F, arrows). Given the critical role of RARγ in the regulation of the Meis1 gene, we further characterized the levels of retinoic acid receptor γ (RARγ) and retinoid receptor α (RXRα) at these three sites (Fig. 5A,B). RARγ levels were slightly elevated in WT versus RARγ$^{-/-}$ cells at all evaluated regions, but showed no specific enrichment at any one particular region. The levels of RXRα at all of these regions were similar to those of IgG (Fig. 5A,B versus Fig. 5F). We detected binding of RXRα at the Cyp26a1 promoter, our positive control (supplementary material Fig. S1), consistent with our previous studies indicating that Cyp26a1 is a direct RA target gene (Kashyap et al., 2011). Consequently, the Meis1 proximal promoter region appears to be devoid of functional RAREs.

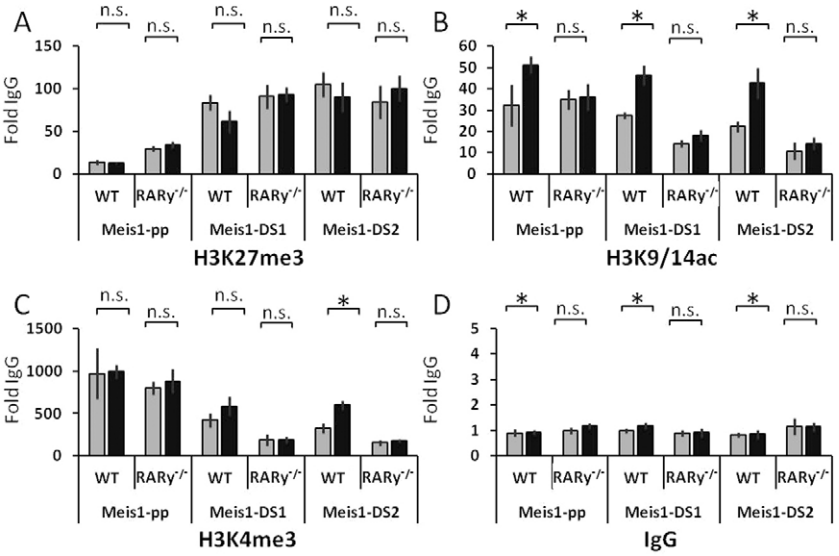

Fig. 4. H3K9/14ac, Suz12, and H3K4me3 associate with specific Meis1 elements. ChIP assays of Meis1 P_{refseq} (pp) and Meis1 downstream elements (DS1 and DS2) in WT and RARγ$^{-/-}$ ES cells evaluating (**A**) H3K9/14ac; (**B**) Suz12; and (**C**) H3K4me3 association with each of the three Meis1 elements. (**D**) IgG was used as a negative control. Each experiment was repeated at least three times, starting with freshly plated cells, and evaluated by quantitative PCR. The data are plotted as fold enrichment relative to IgG background. Note that the y-axes are different in each panel. Values are means ± s.e.m. of three independent experiments. Statistical significance: *$P<0.05$; n.s., not significant. Untreated, gray bars; treated with RA for 24 h, black bars.

Pol II, p300, and histone acetylation are decreased in RARγ knockout cells compared to WT cells

In the WT cells we detected RA induced enrichment of Pol II, most pronounced at the promoter proximal region of Meis1. In contrast to the WT cells, we detected low levels of Pol II in both untreated and RA treated RARγ$^{-/-}$ cells, suggesting that RA fails to increase the levels of Pol II in the RARγ$^{-/-}$ cells (Fig. 5C).

We also assessed the association of the H3K27ac mark and the recruitment of the co-activator p300 (KAT3B) in WT and RARγ$^{-/-}$ ES cells by ChIP. The H3K27ac mark is associated with active enhancers and promoters and this epigenetic mark antagonizes the repressive H3K27me3 mark associated with PcG silencing (Creyghton et al., 2010; Pasini et al., 2010; Vernimmen et al., 2011). In addition, the transcriptional co-activator p300 possesses histone acetyltransferase activity and is recruited to

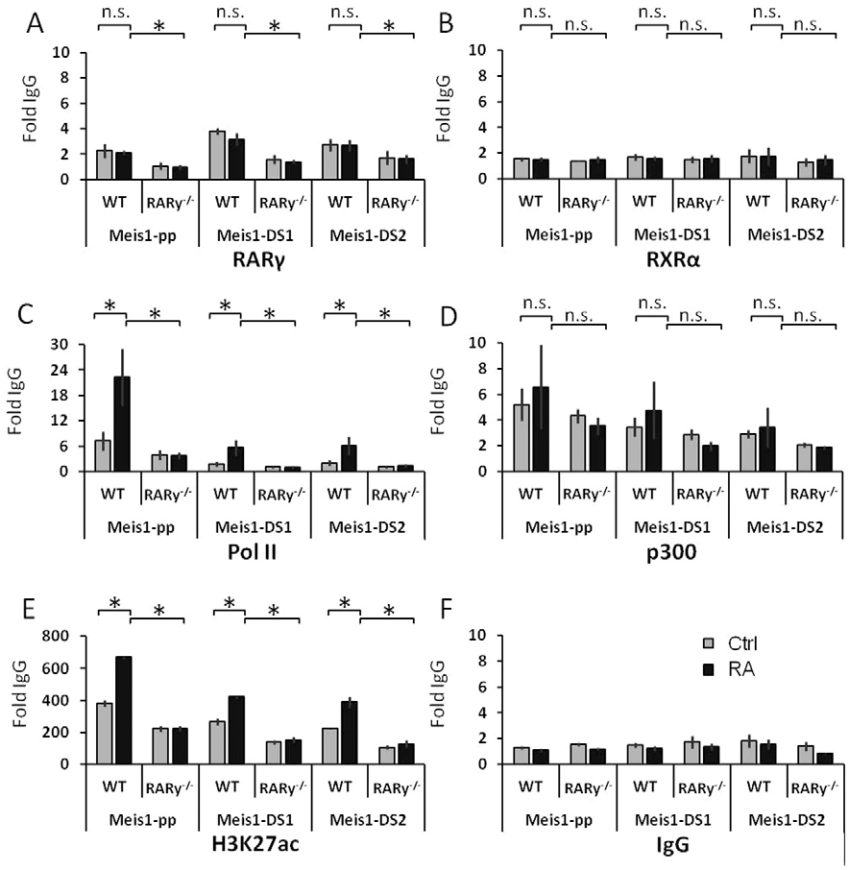

Fig. 5. RARγ, RXRα, H3K27ac, p300, and PolII-CTD association with specific Meis1 elements. ChIP assays of Meis1 P_{refseq} (pp) and Meis1 downstream elements (DS1 and DS2) in WT and RARγ$^{-/-}$ ES cells to evaluate the association of (**A**) RARγ, (**B**) RXRα, (**C**) H3K27ac, (**D**) p300, and (**E**) PolII-CTD with each of the three Meis1 elements. (**F**) IgG was used as a negative control. Each experiment was repeated at least three times, starting with freshly plated cells, and evaluated by quantitative PCR performed in triplicate. The data are plotted as fold enrichment over IgG background. Values are means ± s.e.m. of three independent experiments. Statistical significance: *$P<0.05$; n.s., not significant. Untreated, gray bars; treated with RA for 24 h, black bars.

regulatory enhancer elements in the genome (Heintzman et al., 2009; Visel et al., 2009; Wang et al., 2005). Levels of the H3K27ac mark at the proximal promoter and at the DS1 and DS2 downstream sites of the Meis1 gene increased upon RA treatment of WT, but not RARγ$^{-/-}$ cells (Fig. 5D). We observed low levels of enrichment of p300 at the proximal promoter and the two downstream regions in untreated WT cells. Levels of p300 at the Meis1 gene did not increase significantly with RA treatment, but the levels of both H3K27ac and p300 association were consistently higher in WT compared to RARγ$^{-/-}$ cells (Fig. 5D,E).

RARγ$_2$ is necessary and sufficient for RA induced transcription of Meis1

Because no significant binding of RARγ (or RXRα) was detected in the Meis1 DS1 and DS2 regions identified by the ChIP-chip analysis we decided to further validate the requirement for RARγ. We employed shRNA to deplete RARγ functionally and specifically, thereby providing an independent validation of the RARγ dependent induction of Meis1. The RARγ shRNA knockdown reduced RARγ transcript levels to ~25% of the levels in WT cells, which decreased Meis1 transcript levels to 21% and 45% of the shLuc control with 24 and 48 h of RA treatment, respectively (Fig. 6A). Additionally, we show that knockdown of RARγ by shRNA does not reduce RARα and RARβ transcript levels (supplementary material Fig. S2). These data confirm that RA induces transcription of Meis1 through the actions of RARγ in ES cells.

We next determined if the RA responsiveness of Meis1 can be restored by reintroducing RARγ$_2$, which is the predominantly expressed RARγ isoform. We generated two independent cell lines which ectopically express RARγ$_2$ in the RARγ null background. We then assessed Meis1 mRNA levels in each of the two RARγ$_2$ restoration cell lines (Fig. 6B). We observed Meis1 transcripts in both RARγ$_2$ restoration cell lines relative to the RARγ$^{-/-}$ ES cell line (WT: 19- to 22-fold, clone 1: 10- to 12-fold, and clone 2: 19- to 33-fold, each relative to Meis1 transcript levels in RARγ$^{-/-}$ cells, $P<0.005$ for either treatment condition). Expression of the ectopic RARγ$_2$ cassette was confirmed by assessing RARγ$_2$ transcript levels in the restoration cell lines. The restored RA responsiveness of Meis1 upon ectopic RARγ$_2$ expression demonstrates that RARγ$_2$ is both necessary and sufficient for the RA-associated increase in Meis1 transcripts.

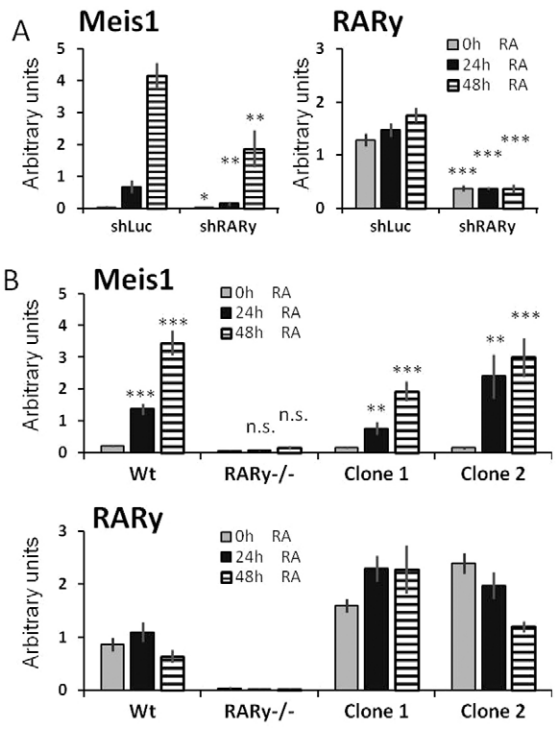

Fig. 6. RARγ knockdown decreases Meis1 transcript levels, and ectopic RARγ$_2$ in RARγ$^{-/-}$ cells restores Meis1 transcript levels. (**A**) In WT ES cells, RARγ knockdown by stable shRNA decreased endogenous Meis1 transcript levels to 21% and 45% upon 24 and 48 h of RA treatment, respectively, as assessed by real time RT-PCR. RARγ transcript levels were reduced to 25% by expression of a RARγ-specific shRNA (shRARγ) relative to a control shRNA targeting luciferase (shLuc). Statistical significance: *$P<0.05$, **$P<0.01$, ***$P<0.005$ relative to WT cells under similar conditions. (**B**) In RARγ$^{-/-}$ ES cells ectopic expression of RARγ$_2$ restored RA responsive levels of Meis1 transcripts. Results are shown from two independent clones (1 and 2). Statistical significance is indicated by *$P<0.05$, **$P<0.01$, ***$P<0.005$ relative to untreated cells.

Discussion

We utilized microarray analysis to identify RARγ regulated genes in WT and RARγ$^{-/-}$ ES cells cultured in the presence versus the absence of RA. The microarray data analysis revealed the important role of RARγ in gene regulation in both the presence of the RA agonist (Fig. 1A; supplementary material Table S4A,B), and in the absence of the ligand, as we observed large numbers of genes that were differentially regulated even in untreated RARγ$^{-/-}$ versus WT ES cells (Fig. 1B; supplementary material Table S2A,B). Additionally, we show that transcript levels of many genes decrease upon 24 h of RA treatment in WT ES cells, thus implicating RA in gene repression (Fig. 1C; supplementary material Table S6B).

The interaction of RARγ with transcription factors and polycomb repressive complexes

The antagonistic, functional cross-talk between RARs and polycomb group (PcG) protein regulated transcription in stem cells has raised many questions concerning the mechanistic details of the recruitment and displacement of the PcG proteins from retinoid regulated genes. It is worth noting that the PcG protein EZH2 has also been shown to associate directly with the repressor of estrogen receptor activity (REA), a co-repressor of ER, and EZH2 repressed estrogen-induced transcription from a reporter (Hwang et al., 2008). These findings call for the identification of co-regulators of RAR mediated transcription that may bind and target PcG proteins to RA target genes in stem cells. We showed that the polycomb protein Suz12 interacts with RARγ in the absence of RA in ES cells and that this interaction is abrogated upon RA addition; however this interaction may not be by direct binding and could be bridged through association with other transcriptional regulators, such as co-repressors (Amat and Gudas, 2011). Importantly, by using the RARγ$^{-/-}$ ES cells we have shown that the lack of RARγ does not interfere with the basal association of the PcG mediated H3K27me3 mark at the Hoxa and Hoxb clusters and other RA targets, such as Cyp26a1 (Kashyap et al., 2011) and Meis1 (Fig. 3F).

Given the differential chromatin signatures and transcript profiles across different cell lineages (Kashyap and Gudas, 2010), it is likely that RARs exhibit cross-talk with other transcription factors in a cell-type dependent manner. In fact, the cell-specific

functions of RARs may be executed in conjunction with transcription factors that play key roles in the biological functions of their respective lineages. The interplay of RARs with other transcription factors, such as Foxa1 (Hua et al., 2009), calls for interrogation and identification of additional transcription factors that may regulate the functions of RARs in ES cells. Some of the transcription factors that we have identified as being transcriptionally activated by RARγ (Figs 1, 3) in ES cells in response to RA are candidates for playing such roles.

RARγ is required for RA-associated epigenetic changes at the Lrat gene

Our data show that RA increases Lrat transcript levels in WT, but not in RARγ$^{-/-}$ cells (Fig. 2A). We show that RARγ is required for the removal of the H3K27me3 mark from the Lrat gene, and that failure to deplete the repressive H3K27me3 mark specifically at the Lrat proximal promoter region is associated with the lack of transcriptional activation by RA in the RARγ$^{-/-}$ cells (Fig. 2F). RARγ is not required for the placement of the H3K4me3 mark and the presence of this mark is not sufficient for Lrat transcriptional activation in RARγ$^{-/-}$ cells (Fig. 2F). We did not detect a DR2 or DR5 RARE within 2 kb 5′ or 3′ of the Lrat start site of transcription, suggesting that Lrat may possess an RARE at some distance from the coding region or that Lrat is a secondary RAR target gene. The absence of H3K9/14ac marks in the Lrat proximal promoter region suggests that RA induction of Lrat is regulated mainly by dissociation of the H3K27me3 repressive mark, a feature which is observed in WT, but not in RARγ$^{-/-}$ cells (Fig. 2F).

Meis1 transcriptional activation by RA involves loss of PcG mediated repression and RARγ mediated epigenetic activation

RA signaling in WT ES cells leads to increased association of the transcriptional activation marks H3K9/14ac at the Meis1 gene, concomitant with increased levels of Pol II (Figs 3–5). These RA dependent epigenetic changes are attenuated or absent in the RARγ$^{-/-}$ cells, in accord with the significantly lower Meis1 transcript levels in RA treated RARγ$^{-/-}$ cells (Figs 3–5). Importantly, we did not find any correlation between placement of the H3K4me3 mark and transcriptional activation of Meis1 by RA. Like the H3K27me3 mark, the H3K4me3 mark is recruited independently of RARγ, thus generating a bivalent domain (Fig. 3F). In this environment in WT cells the activation of RARγ by RA induces local depletion of the H3K27me3 mark, thus shifting the balance between repressive and permissive H3K4me3 histone marks. In addition, the RA induced recruitment of co-activators favors histone acetylation, further potentiating transcriptional induction. We confirmed the requirement for RARγ in the induction of Meis1 through shRARγ depletion of RARγ (Fig. 6A), but we did not detect binding of RARγ or RXRα in the DS1 and DS2 regions of the Meis1 proximal promoter region (Fig. 3F; Fig. 5). This indicates that Meis1 may be an indirect, secondary target of RARγ in ES cells. Alternatively, RAR/RXR binding could occur at an enhancer region distant (+40 kb) from the Meis1 proximal promoter region. The presence of a conserved Pbx1 binding site in the Meis1 proximal promoter region (Magnani et al., 2011) suggests that RARγ may induce Meis1 through or possibly in cooperation with Pbx1.

Conclusions

Our analysis shows that many genes exhibit reduced expression upon RA treatment of WT ES cells; in fact, while 91 genes showed upregulation by RA, 40 genes, including Otx2 and Zfp42, exhibited downregulation by RA at 24 h. This points to non-consensus RA signaling in addition to ligand-induced transcription. Several genes, including DNMT3L, Suv39h1, and Tex13, were differentially expressed between WT and RARγ$^{-/-}$ ES cells independent of RA treatment. Consequently, RARγ may have ligand-independent functions similar to those recently reported for RARα (Laursen et al., 2012). Our research data also lead to novel conclusions about epigenetic modifications of RA-responsive genes in ES cells. First, RARγ is not required for placement of the H3K4me3 epigenetic mark in ES cells and the presence of this mark is not sufficient for transcriptional activation of the RA responsive genes Lrat and Meis1. Additionally, the lack of RARγ increases the association of the H3K27me3 mark with the proximal promoter of Meis1, but not with the downstream elements DS1 and DS2. In conclusion, these data provide new insights into the types of RA induced epigenetic changes in embryonic stem cells.

Materials and Methods

Derivation and culture of the ES cell lines

The cell lines were derived and cultured as described previously (Kashyap et al., 2011). All-trans retinoic acid (RA; Cat. no. 2625, Sigma Chemical Co., MO). RA (1 μM) was added to the cells 24 h after cell-plating and ethanol (0.1%) was used as a vehicle control.

Generation of RARγ knockdown cell lines

Generation of viral particles and transduction of ES cells was previously described (Benoit et al., 2009). In brief, knockdown vectors pLKO shRARγ (hair-pin sequence 5′-CCCAGAGGAAGCCTCTATTTA-3′) or pLKO shLuc (control), together with packaging vectors pCMVΔ8.9 and pVSV-G (Cat. no. 631530, Clontech, CA), were transfected into HEK293T cells using Lipofectamine 2000 (Cat. no. 11668, Invitrogen, CA). After overnight recovery the medium was replaced with fresh medium and the cells were allowed to produce virus for an additional 48 h before the supernatant was harvested, filtered through 0.45 μm filters, and supplemented with polybrene. WT ES cells were transduced with viral supernatant in a 1:1 ratio with 2× growth medium. About 16 h later, the medium was replaced with medium supplemented with puromycin (Cat. no. P7255, Sigma Chemical Co., MO) at a final concentration of 0.5 μg/ml for 10 days of propagation in the selection medium. After this, puromycin was not included in the medium.

Generation of stable clones

The pRosa26-SV40 mRARγ$_2$ expression vector was stably introduced into RARγ$^{-/-}$ ES cells. In brief, the pRosa26 expression vector, which contains a Hygromycin expression cassette was transfected into RARγ$^{-/-}$ ES cells using LTX Plus reagent (Cat. no. 15338, Invitrogen, CA) according to manufacturer's instructions. Selection of stable clones was performed using hygromycin (Cat. no. 10687, Invitrogen, CA) at a final concentration of 100 μg/ml for 10 days. Colonies were picked and screened by PCR using the mRARγE7(+)/mRARγE8(−) primer pair. Successful gDNA purification was evident by a 334 bp PCR product, whereas integration of the transgene was evident by an additional PCR product of 241 bp. Transgene expression in positive clones was verified by the presence of a 162 bp PCR product using the rβ-globin5′C/rβ-globin3′B primer pair, which spans the β-globin intron of the pRosa26-SV40 vector. In addition, the generation of RARγ protein was validated by western blotting (data not shown).

RNA isolation and reverse transcription

Total RNA was extracted using Trizol reagent (Cat. no. 15596, Invitrogen, CA). The RNA was quantitated by optical density at 260 nm. The RNA (1 μg) was reverse transcribed to cDNA using the Quanta reverse transcription mix (Cat. no. 95048, Quanta Biosciences, MD). The cDNA obtained was diluted tenfold and 2 μl of diluted cDNA was utilized for quantitative PCR reactions.

Real time PCR and primers

Real time PCR was carried out in a total volume of 20 μl using the Sybr Green mix (Cat. no. 84091, Quanta Biosciences, MD) according to Kashyap et al. (Kashyap et al., 2011). The primers were designed using the UCSC genome browser (http://genome.ucsc.edu/cgi-bin/hgPc) and all real-time PCR primers were designed

around the introns. The primer sequences can be found in supplementary material Table S1.

Chromatin immunoprecipitation

Cells were treated with RA for 24 h, cross-linked (1% formaldehyde, 10 min), quenched (200 mM glycine, 5 min), washed with ice cold phosphate-buffered saline (PBS), and harvested by scraping. ChIP was performed according to Gillespie and Gudas (Gillespie and Gudas, 2007a; Gillespie and Gudas, 2007b). At least three biological replicate ChIP experiments were performed.

Antibodies and chemicals

Anti-H3K27ac (07-360), anti-H3K4me3 (07-473) and anti-H3K9/14ac (06–599) antibodies were purchased from Millipore (Billerica, MA). Anti-RXRα (D-20, sc-553), anti-p300 (N-15, sc-584), and anti-IgG (sc-2030) antibodies were purchased from Santa Cruz Biotechnology (Santa Cruz, CA). Anti-phospho-Ser-5 carboxyl-terminal domain (CTD) of RNA polymerase II (pCTDser5) was purchased from Covance Research Products (Richmond, CA). Anti-RARγ (ab12012) and Anti-H3K27me3 (ab6002) were purchased from Abcam Inc. (Cambridge, MA).

Microarray expression profiling and analysis

Cells were treated with RA for various times (0, 8 and 24 h) prior to harvesting. Total RNA was isolated using Trizol. RNA quality was assessed using the RNA 6000 NanoAssay and a Bioanalyzer 2100 (Agilent). Samples with a 28S/18S ribosomal peak ratio of 1.8–2.0 were considered suitable for labeling. 200 ng of total RNA from each sample was labeled using the Illumina Total Prep RNA Amplification kit (Ambion), according to the manufacturer's instructions. Labeled and fragmented cRNAs (3 µg) were then hybridized to the mouse-ref8 array (Illumina), which incorporates 22,000 transcripts of known mouse genes. The raw data obtained from the Illumina microarray platform were imported into Genespring 11 (Agilent) and were normalized using the quantile normalization procedure. Following the normalization, the data were filtered for expression values. The data across replicates were averaged and subsequently, the list of genes that showed statistically significant fold changes ($P<0.05$) was obtained. The generation of the ChIP-chip data has been previously described (Kashyap et al., 2011). We obtained bioinformatics advice on data analyses from Dr Piali Mukherjee at the Epigenomics Core at Weill Cornell Medical College. Gene expression profiles were deposited at GEO with the accession code GSE43221 (http://www.ncbi.nlm.nih.gov/geo/query/acc.cgi?acc=GSE43221).

Acknowledgements

We thank members of the Gudas laboratory for helpful discussions about this research. We thank Dr Pierre Chambon for the RARγ knockout mice. We thank Tamara Weissman for editorial assistance in the preparation of this manuscript.

Author contributions

V.K., K.B.L., F.B., A.J.V., and J.M.S. performed experiments. V.K., K.B.L., J.M.S., and L.J.G. wrote the manuscript. V.K., K.B.L., A.J.V., J.M.S., and L.J.G. analyzed and interpreted the data.

Funding

This research was supported by National Institutes of Health [grant number NIH R01 CA043796 to L.J.G.]; and Weill Cornell funds [to L.J.G.]. Deposited in PMC for release after 12 months.

Supplementary material available online at
http://jcs.biologists.org/lookup/suppl/doi:10.1242/jcs.119701/-/DC1

References

Amat, R. and Gudas, L. J. (2011). RARγ is required for correct deposition and removal of Suz12 and H2A.Z in embryonic stem cells. *J. Cell. Physiol.* **226**, 293-298.

Amengual, J., Golczak, M., Palczewski, K. and von Lintig, J. (2012). Lecithin:retinol acyltransferase is critical for cellular uptake of vitamin A from serum retinol-binding protein. *J. Biol. Chem.* **287**, 24216-24227.

Azcoitia, V., Aracil, M., Martínez-A, C. and Torres, M. (2005). The homeodomain protein Meis1 is essential for definitive hematopoiesis and vascular patterning in the mouse embryo. *Dev. Biol.* **280**, 307-320.

Batten, M. L., Imanishi, Y., Maeda, T., Tu, D. C., Moise, A. R., Bronson, D., Possin, D., Van Gelder, R. N., Baehr, W. and Palczewski, K. (2004). Lecithin-retinol acyltransferase is essential for accumulation of all-trans-retinyl esters in the eye and in the liver. *J. Biol. Chem.* **279**, 10422-10432.

Bayha, E., Jørgensen, M. C., Serup, P. and Grapin-Botton, A. (2009). Retinoic acid signaling organizes endodermal organ specification along the entire antero-posterior axis. *PLoS ONE* **4**, e5845.

Benoit, Y. D., Lussier, C., Ducharme, P. A., Sivret, S., Schnapp, L. M., Basora, N. and Beaulieu, J. F. (2009). Integrin alpha8beta1 regulates adhesion, migration and proliferation of human intestinal crypt cells via a predominant RhoA/ROCK-dependent mechanism. *Biol. Cell* **101**, 695-708.

Berry, D. C., Jin, H., Majumdar, A. and Noy, N. (2011). Signaling by vitamin A and retinol-binding protein regulates gene expression to inhibit insulin responses. *Proc. Natl. Acad. Sci. USA* **108**, 4340-4345.

Boyer, L. A., Plath, K., Zeitlinger, J., Brambrink, T., Medeiros, L. A., Lee, T. I., Levine, S. S., Wernig, M., Tajonar, A., Ray, M. K. et al. (2006). Polycomb complexes repress developmental regulators in murine embryonic stem cells. *Nature* **441**, 349-353.

Boylan, J. F., Lohnes, D., Taneja, R., Chambon, P. and Gudas, L. J. (1993). Loss of retinoic acid receptor gamma function in F9 cells by gene disruption results in aberrant Hoxa-1 expression and differentiation upon retinoic acid treatment. *Proc. Natl. Acad. Sci. USA* **90**, 9601-9605.

Boylan, J. F., Lufkin, T., Achkar, C. C., Taneja, R., Chambon, P. and Gudas, L. J. (1995). Targeted disruption of retinoic acid receptor alpha (RAR alpha) and RAR gamma results in receptor-specific alterations in retinoic acid-mediated differentiation and retinoic acid metabolism. *Mol. Cell. Biol.* **15**, 843-851.

Chang, C. P., Brocchieri, L., Shen, W. F., Largman, C. and Cleary, M. L. (1996). Pbx modulation of Hox homeodomain amino-terminal arms establishes different DNA-binding specificities across the Hox locus. *Mol. Cell. Biol.* **16**, 1734-1745.

Chen, C. F., Goyette, P. and Lohnes, D. (2004). RARgamma acts as a tumor suppressor in mouse keratinocytes. *Oncogene* **23**, 5350-5359.

Clagett-Dame, M. and Knutson, D. (2011). Vitamin A in reproduction and development. *Nutrients* **3**, 385-428.

Creyghton, M. P., Cheng, A. W., Welstead, G. G., Kooistra, T., Carey, B. W., Steine, E. J., Hanna, J., Lodato, M. A., Frampton, G. M., Sharp, P. A. et al. (2010). Histone H3K27ac separates active from poised enhancers and predicts developmental state. *Proc. Natl. Acad. Sci. USA* **107**, 21931-21936.

Eklund, E. A. (2007). The role of HOX genes in malignant myeloid disease. *Curr. Opin. Hematol.* **14**, 85-89.

Featherstone, M. (2003). HOX proteins and their co-factors in transcriptional regulation. In *Advances in Developmental Biology and Biochemistry,* Vol. 13, pp. 1-42.

Gavalas, A., Ruhrberg, C., Livet, J., Henderson, C. E. and Krumlauf, R. (2003). Neuronal defects in the hindbrain of Hoxa1, Hoxb1 and Hoxb2 mutants reflect regulatory interactions among these Hox genes. *Development* **130**, 5663-5679.

Gillespie, R. F. and Gudas, L. J. (2007a). Retinoic acid receptor isotype specificity in F9 teratocarcinoma stem cells results from the differential recruitment of coregulators to retinoic response elements. *J. Biol. Chem.* **282**, 33421-33434.

Gillespie, R. F. and Gudas, L. J. (2007b). Retinoid regulated association of transcriptional co-regulators and the polycomb group protein SUZ12 with the retinoic acid response elements of Hoxa1, RARbeta(2), and Cyp26A1 in F9 embryonal carcinoma cells. *J. Mol. Biol.* **372**, 298-316.

Golzio, C., Martinovic-Bouriel, J., Thomas, S., Mougou-Zrelli, S., Grattagliano-Bessieres, B., Bonniere, M., Delahaye, S., Munnich, A., Encha-Razavi, F., Lyonnet, S. et al. (2007). Matthew-Wood syndrome is caused by truncating mutations in the retinol-binding protein receptor gene STRA6. *Am. J. Hum. Genet.* **80**, 1179-1187.

Goyette, P., Feng Chen, C., Wang, W., Seguin, F. and Lohnes, D. (2000). Characterization of retinoic acid receptor-deficient keratinocytes. *J. Biol. Chem.* **275**, 16497-16505.

Gudas, L. J. and Wagner, J. A. (2011). Retinoids regulate stem cell differentiation. *J. Cell. Physiol.* **226**, 322-330.

Guo, X. and Gudas, L. J. (1998). Metabolism of all-trans-retinol in normal human cell strains and squamous cell carcinoma (SCC) lines from the oral cavity and skin: reduced esterification of retinol in SCC lines. *Cancer Res.* **58**, 166-176.

Heintzman, N. D., Hon, G. C., Hawkins, R. D., Kheradpour, P., Stark, A., Harp, L. F., Ye, Z., Lee, L. K., Stuart, R. K., Ching, C. W. et al. (2009). Histone modifications at human enhancers reflect global cell-type-specific gene expression. *Nature* **459**, 108-112.

Hisa, T., Spence, S. E., Rachel, R. A., Fujita, M., Nakamura, T., Ward, J. M., Devor-Henneman, D. E., Saiki, Y., Kutsuna, H., Tessarollo, L. et al. (2004). Hematopoietic, angiogenic and eye defects in Meis1 mutant animals. *EMBO J.* **23**, 450-459.

Hua, S., Kittler, R. and White, K. P. (2009). Genomic antagonism between retinoic acid and estrogen signaling in breast cancer. *Cell* **137**, 1259-1271.

Hwang, C., Giri, V. N., Wilkinson, J. C., Wright, C. W., Wilkinson, A. S., Cooney, K. A. and Duckett, C. S. (2008). EZH2 regulates the transcription of estrogen-responsive genes through association with REA, an estrogen receptor corepressor. *Breast Cancer Res. Treat.* **107**, 235-242.

Jenuwein, T. and Allis, C. D. (2001). Translating the histone code. *Science* **293**, 1074-1080.

Kashyap, V. and Gudas, L. J. (2010). Epigenetic regulatory mechanisms distinguish retinoic acid-mediated transcriptional responses in stem cells and fibroblasts. *J. Biol. Chem.* **285**, 14534-14548.

Kashyap, V., Gudas, L. J., Brenet, F., Funk, P., Viale, A. and Scandura, J. M. (2011). Epigenomic reorganization of the clustered Hox genes in embryonic stem cells induced by retinoic acid. *J. Biol. Chem.* **286**, 3250-3260.

Kawagoe, H., Humphries, R. K., Blair, A., Sutherland, H. J. and Hogge, D. E. (1999). Expression of HOX genes, HOX cofactors, and MLL in phenotypically and functionally defined subpopulations of leukemic and normal human hematopoietic cells. *Leukemia* **13**, 687-698.

Kawaguchi, R., Yu, J., Honda, J., Hu, J., Whitelegge, J., Ping, P., Wiita, P., Bok, D. and Sun, H. (2007). A membrane receptor for retinol binding protein mediates cellular uptake of vitamin A. *Science* **315**, 820-825.

Kreidberg, J. A., Sariola, H., Loring, J. M., Maeda, M., Pelletier, J., Housman, D. and Jaenisch, R. (1993). WT-1 is required for early kidney development. *Cell* **74**, 679-691.

Langton, S. and Gudas, L. J. (2008). CYP26A1 knockout embryonic stem cells exhibit reduced differentiation and growth arrest in response to retinoic acid. *Dev. Biol.* **315**, 331-354.

Laursen, K. B., Wong, P. M. and Gudas, L. J. (2012). Epigenetic regulation by RARα maintains ligand-independent transcriptional activity. *Nucleic Acids Res.* **40**, 102-115.

Lin, Z., Cantos, R., Patente, M. and Wu, D. K. (2005). Gbx2 is required for the morphogenesis of the mouse inner ear: a downstream candidate of hindbrain signaling. *Development* **132**, 2309-2318.

Liu, L. and Gudas, L. J. (2005). Disruption of the lecithin:retinol acyltransferase gene makes mice more susceptible to vitamin A deficiency. *J. Biol. Chem.* **280**, 40226-40234.

Lohnes, D., Kastner, P., Dierich, A., Mark, M., LeMeur, M. and Chambon, P. (1993). Function of retinoic acid receptor gamma in the mouse. *Cell* **73**, 643-658.

Magnani, L., Ballantyne, E. B., Zhang, X. and Lupien, M. (2011). PBX1 genomic pioneer function drives ERα signaling underlying progression in breast cancer. *PLoS Genet.* **7**, e1002368.

Makarenkova, H. P. and Meech, R. (2012). Barx homeobox family in muscle development and regeneration. *Int. Rev. Cell Mol. Biol.* **297**, 117-173.

Mark, M., Ghyselinck, N. B. and Chambon, P. (2009). Function of retinoic acid receptors during embryonic development. *Nucl. Recept. Signal.* **7**, e002.

McGowan, S., Jackson, S. K., Jenkins-Moore, M., Dai, H. H., Chambon, P. and Snyder, J. M. (2000). Mice bearing deletions of retinoic acid receptors demonstrate reduced lung elastin and alveolar numbers. *Am. J. Respir. Cell Mol. Biol.* **23**, 162-167.

Means, A. L. and Gudas, L. J. (1995). The roles of retinoids in vertebrate development. *Annu. Rev. Biochem.* **64**, 201-233.

Meister, B., Fink, F. M., Hittmair, A., Marth, C. and Widschwendter, M. (1998). Antiproliferative activity and apoptosis induced by retinoic acid receptor-gamma selectively binding retinoids in neuroblastoma. *Anticancer Res.* **18**, 1777-1786.

Moens, C. B. and Selleri, L. (2006). Hox cofactors in vertebrate development. *Dev. Biol.* **291**, 193-206.

Noy, N. (2000). Retinoid-binding proteins: mediators of retinoid action. *Biochem. J.* **348**, 481-495.

O'Byrne, S. M., Wongsiriroj, N., Libien, J., Vogel, S., Goldberg, I. J., Baehr, W., Palczewski, K. and Blaner, W. S. (2005). Retinoid absorption and storage is impaired in mice lacking lecithin:retinol acyltransferase (LRAT). *J. Biol. Chem.* **280**, 35647-35657.

Pasini, D., Malatesta, M., Jung, H. R., Walfridsson, J., Willer, A., Olsson, L., Skotte, J., Wutz, A., Porse, B., Jensen, O. N. et al. (2010). Characterization of an antagonistic switch between histone H3 lysine 27 methylation and acetylation in the transcriptional regulation of Polycomb group target genes. *Nucleic Acids Res.* **38**, 4958-4969.

Pasutto, F., Sticht, H., Hammersen, G., Gillessen-Kaesbach, G., Fitzpatrick, D. R., Nürnberg, G., Brasch, F., Schirmer-Zimmermann, H., Tolmie, J. L., Chitayat, D. et al. (2007). Mutations in STRA6 cause a broad spectrum of malformations including anophthalmia, congenital heart defects, diaphragmatic hernia, alveolar capillary dysplasia, lung hypoplasia, and mental retardation. *Am. J. Hum. Genet.* **80**, 550-560.

Pelletier, J., Bruening, W., Li, F. P., Haber, D. A., Glaser, T. and Housman, D. E. (1991a). WT1 mutations contribute to abnormal genital system development and hereditary Wilms' tumour. *Nature* **353**, 431-434.

Pelletier, J., Schalling, M., Buckler, A. J., Rogers, A., Haber, D. A. and Housman, D. (1991b). Expression of the Wilms' tumor gene WT1 in the murine urogenital system. *Genes Dev.* **5**, 1345-1356.

Purton, L. E. (2007). Roles of retinoids and retinoic acid receptors in the regulation of hematopoietic stem cell self-renewal and differentiation. *PPAR Res.* **2007**, 87934.

Purton, L. E., Dworkin, S., Olsen, G. H., Walkley, C. R., Fabb, S. A., Collins, S. J. and Chambon, P. (2006). RARgamma is critical for maintaining a balance between hematopoietic stem cell self-renewal and differentiation. *J. Exp. Med.* **203**, 1283-1293.

Samarut, E. and Rochette-Egly, C. (2012). Nuclear retinoic acid receptors: conductors of the retinoic acid symphony during development. *Mol. Cell. Endocrinol.* **348**, 348-360.

Shanmugam, K., Green, N. C., Rambaldi, I., Saragovi, H. U. and Featherstone, M. S. (1999). PBX and MEIS as non-DNA-binding partners in trimeric complexes with HOX proteins. *Mol. Cell. Biol.* **19**, 7577-7588.

Shen, W. F., Chang, C. P., Rozenfeld, S., Sauvageau, G., Humphries, R. K., Lu, M., Lawrence, H. J., Cleary, M. L. and Largman, C. (1996). Hox homeodomain proteins exhibit selective complex stabilities with Pbx and DNA. *Nucleic Acids Res.* **24**, 898-906.

Shen, W. F., Montgomery, J. C., Rozenfeld, S., Moskow, J. J., Lawrence, H. J., Buchberg, A. M. and Largman, C. (1997). AbdB-like Hox proteins stabilize DNA binding by the Meis1 homeodomain proteins. *Mol. Cell. Biol.* **17**, 6448-6458.

Sims, R. J., 3rd and Reinberg, D. (2006). Histone H3 Lys 4 methylation: caught in a bind? *Genes Dev.* **20**, 2779-2786.

Smith, A. G. (2001). Embryo-derived stem cells: of mice and men. *Annu. Rev. Cell Dev. Biol.* **17**, 435-462.

Soprano, D. R., Teets, B. W. and Soprano, K. J. (2007). Role of retinoic acid in the differentiation of embryonal carcinoma and embryonic stem cells. *Vitam. Horm.* **75**, 69-95.

Spanjaard, R. A., Ikeda, M., Lee, P. J., Charpentier, B., Chin, W. W. and Eberlein, T. J. (1997). Specific activation of retinoic acid receptors (RARs) and retinoid X receptors reveals a unique role for RARgamma in induction of differentiation and apoptosis of S91 melanoma cells. *J. Biol. Chem.* **272**, 18990-18999.

Su, D. and Gudas, L. J. (2008a). Gene expression profiling elucidates a specific role for RARgamma in the retinoic acid-induced differentiation of F9 teratocarcinoma stem cells. *Biochem. Pharmacol.* **75**, 1129-1160.

Su, D. and Gudas, L. J. (2008b). Retinoic acid receptor gamma activates receptor tyrosine kinase Tie1 gene transcription through transcription factor GATA4 in F9 stem cells. *Exp. Hematol.* **36**, 624-641.

Vernimmen, D., Lynch, M. D., De Gobbi, M., Garrick, D., Sharpe, J. A., Sloane-Stanley, J. A., Smith, A. J. and Higgs, D. R. (2011). Polycomb eviction as a new distant enhancer function. *Genes Dev.* **25**, 1583-1588.

Visel, A., Blow, M. J., Li, Z., Zhang, T., Akiyama, J. A., Holt, A., Plajzer-Frick, I., Shoukry, M., Wright, C., Chen, F. et al. (2009). ChIP-seq accurately predicts tissue-specific activity of enhancers. *Nature* **457**, 854-858.

Wang, Q., Carroll, J. S. and Brown, M. (2005). Spatial and temporal recruitment of androgen receptor and its coactivators involves chromosomal looping and polymerase tracking. *Mol. Cell* **19**, 631-642.

Wang, G. G., Pasillas, M. P. and Kamps, M. P. (2006). Persistent transactivation by meis1 replaces hox function in myeloid leukemogenesis models: evidence for co-occupancy of meis1-pbx and hox-pbx complexes on promoters of leukemia-associated genes. *Mol. Cell. Biol.* **26**, 3902-3916.

Wassarman, K. M., Lewandoski, M., Campbell, K., Joyner, A. L., Rubenstein, J. L., Martinez, S. and Martin, G. R. (1997). Specification of the anterior hindbrain and establishment of a normal mid/hindbrain organizer is dependent on Gbx2 gene function. *Development* **124**, 2923-2934.

Wendling, O., Ghyselinck, N. B., Chambon, P. and Mark, M. (2001). Roles of retinoic acid receptors in early embryonic morphogenesis and hindbrain patterning. *Development* **128**, 2031-2038.

White, J. A., Beckett-Jones, B., Guo, Y. D., Dilworth, F. J., Bonasoro, J., Jones, G. and Petkovich, M. (1997). cDNA cloning of human retinoic acid-metabolizing enzyme (hP450RAI) identifies a novel family of cytochromes P450. *J. Biol. Chem.* **272**, 18538-18541.

Williams, J. A., Kondo, N., Okabe, T., Takeshita, N., Pilchak, D. M., Koyama, E., Ochiai, T., Jensen, D., Chu, M. L., Kane, M. A. et al. (2009). Retinoic acid receptors are required for skeletal growth, matrix homeostasis and growth plate function in postnatal mouse. *Dev. Biol.* **328**, 315-327.

Wong, P., Iwasaki, M., Somervaille, T. C., So, C. W. and Cleary, M. L. (2007). Meis1 is an essential and rate-limiting regulator of MLL leukemia stem cell potential. *Genes Dev.* **21**, 2762-2774.

Wu, M., Zhang, Y., Wu, N. H. and Shen, Y. F. (2009). Histone marks and chromatin remodelers on the regulation of neurogenin1 gene in RA induced neuronal differentiation of P19 cells. *J. Cell. Biochem.* **107**, 264-271.

Zolfaghari, R. and Ross, A. C. (2000). Lecithin:retinol acyltransferase from mouse and rat liver. CDNA cloning and liver-specific regulation by dietary vitamin a and retinoic acid. *J. Lipid Res.* **41**, 2024-2034.

SUPPLEMENTAL FIGURES

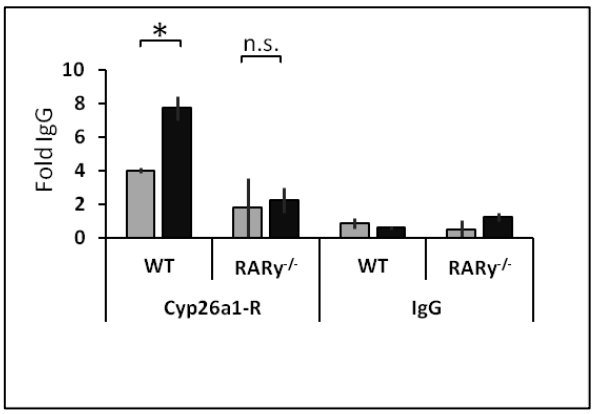

Fig. S1. RXRα association with Cyp26a1 RARE. ChIP assays of Cyp26a1 RARE (Cyp26a1-R) in WT and RARγKO ES cells evaluating RARγ association. IgG served as negative control. Statistical significance is indicated by * ($p<0.05$); n.s. – not significant. Untreated, grey bars (■); treated with RA for 24 hr, black bars (■).

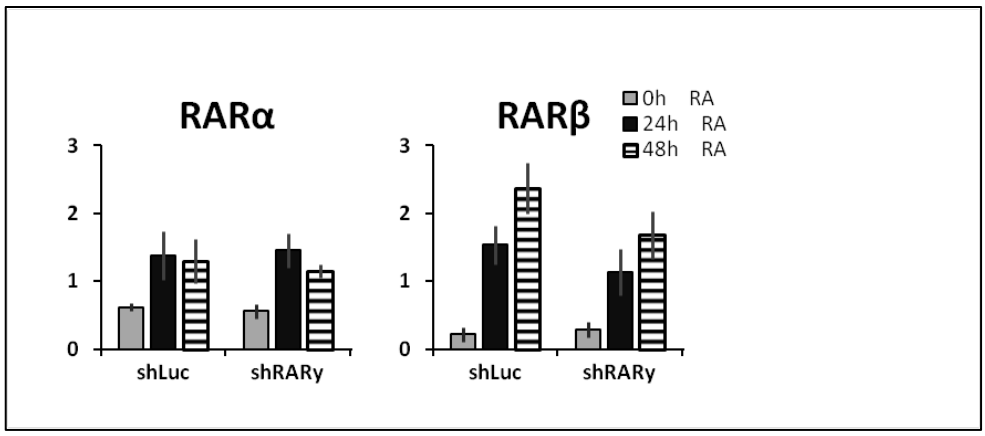

Fig. S2. RARγ knockdown does not affect RARα and RARβ expression. In ES cells, RARγ knockdown had no effect on RARα transcript level. Furthermore, RA potently increased the levels of RARβ transcript even upon RARγ depletion. This shows not only that the shRNA is specific for RARγ, but also that induction of RARβ by RA does not depend on RARγ. The effects of the RARγ-specific shRNA (shRARγ) are depicted relative to a control shRNA targeting luciferase (shLuc).

SUPPLEMENTAL TABLES

Table 1: Primer Sequences

Target	Sequence
RT-PCR	
36B4F	5' AGAACAACCCAGCTCTGGAGAAA 3'
36B4R	5' ACACCCTCCAGAAAGCGAGAGT 3'
Barx1F	5' CGAGCTGCTCAAGTTCGG 3'
Barx1R	5' GTGGGAACTTGAACACTGCG 3'
Crabp2F	5' TTCTGGCAACTGGAAGATCATCCG 3'
Crabp2R	5' ATCATTGGTCAGTTCTCGGCTCCA 3'
Cyp26a1F	5' GAAACATTGCAGATGGTGCTTCAG 3'
Cyp26a1R	5' CGGCTGAAGGCCTGCATAATCAC 3'
Gbx2F	5' GGCAACTTCGACAAAGCCGAGG 3'
Gbx2R	5' CCAGGCAAATTGTCATCTGAGC 3'
LratF	5' GACTTACTGCAGATATGGCTCTCG 3'
LratR	5' ATGGGATACAGATTGCAGGAAGGG 3'
Meis1F	5' CATGATAGACCAGTCCAACC 3'
Meis1R	5'GGCTACATACTCCCCTGGCATACT 3' 3'
Pbx1F	5' GGACATCGGGGACATTTTACAGCA 3'
Pbx1R	5' GCATGTTGTCCAGTCGCATGAGC 3'
RARαF	5' TGGCTCAAACCACTCCATCGAGA 3'
RARαR	5' CCTGGTGCGCTTTGCGAACC 3'
RARβF	5' GCAGCACCGGCATACTGCTC 3'
RARβR	5' GTAGCCCGATGACTTGTCCTG 3'
RARγF	5' TGCCAGTCTACAATCGGTGGA 3'
RARγR	5' GATACAGTTTTTGTCACGGTGACAT 3'
Stra6F	5' GTTCAGGTCTGGCAGAAAGC 3'
Stra6R	5' CAGGAATCCAAGACCCAGAA 3'
Wt1F	5' GCCTTCACCTTGCACTTCTC 3'
Wt1R	5' GACCGTGCTGTATCCTTGGT 3'
ChIP	
Cyp26a1R-F	5' TTCACTGAGATGTCACGGTCC 3'
Cyp26a1R-R	5' TTCCCAATCCTTTAGCCTGA 3'
Meis1 DS II	5' TCCCTCTGACTTTATTGT 3'
Meis1 DS II	5' CATTGATTGTTCTGACTTG 3'
Meis1 DS I	5' CAGTGCTAAGAGAGGGAAGA 3'
Meis1 DS I	5' TCTGGACTAATCATTGTGTTGTT 3'
Meis1 PP R	5' ACTCTTCAGCTACTCTATC 3'
Meis1 PP F	5' TGTGACTGAGCAATCTAA 3'
Genotyping	
mRARγE7(+)	5'CCCCCGACAGCTATGAACTGA 3'
mRARγE8(-)	5'GCAATGCTGAGCCCTGTAAAACCA 3'
rβ-globin3'B	5'CGCCCTATAGTGAGTCGTATTACA 3'
rβ-globin5'C	5'TATTCCAGAAGTAGTGAGGAGGC 3'

Table 2A: Transcripts that were lower by 3-fold or more in untreated RARγ KO ES cells compared to untreated WT ES cells (a total of 80 transcripts)

Probe ID	Fold decrease [RARγ KO-0] vs [WT-0]	Symbol	Entrez Gene ID	Definition
6960730	42.35	Eif2s3y	26908	Eukaryotic translation initiation factor 2, subunit 3 structural gene Y-linked
6350678	11.69	Gata6	14465	GATA binding protein 6
5290711	8.96	Car2	12349	Carbonic anhydrase 2
4070142	8.67	Gadd45g	23882	Growth arrest and DNA-damage-inducible 45 gamma
4890402	7.79	Tesk1	21754	Testis specific protein kinase 1
1850487	7.25	Foxq1	15220	Forkhead box Q1
3610347	7.13	Fbp2	14120	Fructose bisphosphatase 2
4760255	7.13	A130072J07	240832	Torsin A interacting protein 2 (Tor1aip2)
1450408	7.08	6330407J23Rik	67412	6330407J23Rik RIKEN cdna 6330407J23 gene
4060102	7.03	Col4a1	12826	Procollagen, type IV, alpha 1
1660703	6.94	Wt1	22431	Wilms tumor 1 homolog
7320056	6.74	Bat5	193742	Abhydrolase domain containing 16A
1500286	6.72	Car4	12351	Carbonic anhydrase 4
5130528	6.35	MGC117846	626316	Predicted gene
870484	5.87	4930455C21Rik	76916	RIKEN cdna 4930455C21 gene
1820746	5.81	Pitx2	18741	Paired-like homeodomain transcription factor 2 transcript variant 3
4860719	5.77	Myo1f	17916	Myosin IF
2260551	5.59	Col4a2	12827	Procollagen, type IV, alpha 2
270274	5.52	Rpo1-4	20019	Polymerase (RNA) I polypeptide A
3060546	5.45	Dpp4	13482	Dipeptidylpeptidase 4
3060470	5.19	Peg10	170676	Paternally expressed 10, transcript variant 1
1050609	5.11	Dab2	13132	Disabled homolog 2 (Drosophila) transcript variant 2
1940347	4.72	Dab2	13132	Disabled homolog 2 (Drosophila) transcript variant 2
3940242	4.61	AA175286	209086	Sterile alpha motif domain containing 9-like
4480180	4.60	Phlda1	21664	Pleckstrin homology-like domain, family A, member 1
430451	4.35	Mmrn2	105450	Multimerin 2
5290521	4.28	Pdgfra	18595	Platelet derived growth factor receptor, alpha polypeptide
3450719	4.19	Mbnl2	105559	Muscleblind-like 2 transcript variant 2
5670554	4.15	2300002G24Rik	74175	Cysteine-rich C-terminal 1 (Crct1)
4050400	4.09	Zyx	2279	Zyxin
670360	4.09	2310057H16Rik	67951	Tubulin, beta 6 (Tubb6)
7320338	4.02	Pitx2	18741	Paired-like homeodomain transcription factor 2, transcript variant 3
3170326	4.01	Scarf2	224024	Scavenger receptor class F, member 2
2230687	3.96	Nope	56741	Neighbor of Punc E11
3850326	3.94	Itgb4	192897	Integrin beta 4
4730685	3.80	Pmp22	18858	Peripheral myelin protein 22
4640114	3.79	Actb	11461	Actin, beta, cytoplasmic
3610619	3.78	Nt5e	23959	5' nucleotidase, ecto

70386	3.59	Satb1	20230	Special AT-rich sequence binding protein 1
160079	3.59	LOC626391	626391	Similar to Zinc finger protein 124 (HZF-16)
7560647	3.57	Meis1	17268	Meis homeobox 1
2710142	3.56	Mbnl2	105559	Muscleblind-like 2 transcript variant 1
1010050	3.54	Lmo4	16911	LIM domain only 4
3140274	3.52	Dcxr	67880	Dicarbonyl L-xylulose reductase
240373	3.51	D14Ertd449e	66039	DNA segment, Chr 14, ERATO Doi 449, expressed
1340328	3.47	LOC381813	381813	Protein arginine N-methyltransferase 8 (Prmt8)
7320646	3.47	Tal2	21350	T-cell acute lymphocytic leukemia 2
5420309	3.41	1200009O22Rik	66873	RIKEN cdna 1200009O22 gene
2680722	3.38	Actb	11461	Actin, beta, cytoplasmic
4050670	3.35	Efnb2	13642	Ephrin b2
2900692	3.33	Has2	15117	Hyaluronan synthase 2
1940142	3.33	Steap	70358	Six transmembrane epithelial antigen of the prostate1
1190465	3.31	Rusc2	100213	Run and sh3 domain containing 2, transcript variant 1
4880187	3.31	Erdr1	170942	Erythroid differentiation regulator 1
6370520	3.30	Tnfrsf25	85030	Tumor necrosis factor receptor superfamily, member 25
780386	3.29	Actb	11461	Actin, beta, cytoplasmic
6040445	3.29	Tcte3	21647	T-complex-associated testis expressed 3, transcript variant 2
10703	3.27	Gm397	245109	Gene model 397
10739	3.25	Rg9mtd1	52575	Rna (guanine-9-) methyltransferase domain containing 1
7320053	3.25	Gpx3	14778	Glutathione peroxidase 3
50079	3.23	Hist1h1c	50708	Histone Cluster 1, h1c
6380379	3.23	Pon2	330260	Paraoxonase 2
610092	3.22	Grm6	108072	Glutamate receptor, metabotropic 6
2230026	3.17	9130213B05Rik	231440	Prostate androgen-regulated mucin-like protein 1
4730255	3.16	Galnt11	231050	Udp-n-acetyl-alpha-d-galactosamine:polypeptide n-acetylgalactosaminyltransferase 11
2360521	3.15	AA792894	57896	Krcc1 lysine-rich coiled-coil 1
6380634	3.14	Zfhx2	239102	Zinc finger homeobox 2
4760458	3.13	Ssbp4	76900	Single stranded dna binding protein 4
5270279	3.10	Alox5ap	11690	Arachidonate 5-lipoxygenase activating protein
430368	3.07	4732496O08Rik	242736	Riken cdna 4732496o08 gene
1580519	3.07	Anxa3	11745	Annexin a3
460682	3.06	2200001I15Rik	69134	Riken cdna 2200001i15 gene
6580731	3.05	Prmt2	15468	Protein arginine n-methyltransferase 2 transcript variant 2
1090328	3.05	Suv39h1	20937	Suppressor of variegation 3-9 homolog 1 (Drosophila)
2680739	3.04	Farp1	223254	Farp1 ferm, rhogef (arhgef) and pleckstrin domain protein 1 (chondrocyte-derived)
4250059	3.04	Notch4	18132	Notch gene homolog 4 (drosophila)
6550082	3.04	Lamb1-1	16777	Laminin b1

4560280	3.03	2600001B17Rik	268490	Lsm12 homolog (s. Cerevisiae)
4490445	3.03	Hs3st1	15476	Heparan sulfate (glucosamine) 3-o-sulfotransferase 1
6860048	3.02	Taf7l	74469	Taf7-like rna polymerase ii tata box binding protein (tbp)-associated factor

Table 2B: Transcripts that were higher by 3-fold or more in untreated RARγ KO ES cells compared to untreated WT ES cells (a total of 78 transcripts)

Probe ID	Fold increase [RARγKO-0] vs [WT-0]	Symbol	Entrez Gene ID	Definition
4880603	40.03	Barx1	12022	Barh-like homeobox 1
520427	21.15	Plk1	18817	Polo-like kinase 1
2940164	12.51	Rbm13	67920	RNA binding motif protein 13
1780341	10.05	Krt1-17	16667	Keratin 17
2650131	9.18	Rarb	218772	Retinoic acid receptor beta
7100301	7.23	2810417H13Rik	68026	RIKEN cdna 2810417H13 gene
6060433	7.02	Gjb3	14620	Gap junction membrane channel protein beta 3
2100333	6.36	Lrrc57	66606	Leucine rich repeat containing 57
990672	6.35	Fbxl3a	50789	F-box and leucine-rich repeat protein 3
6060730	6.35	Lars2	102436	Leucyl-trna synthetase, mitochondrial
1300202	6.10	Eprs	107508	Glutamyl-prolyl-trna synthetase
5290360	5.81	Picalm	233489	Picalm phosphatidylinositol binding clathrin assembly protein
7380142	5.71	Snx5	69178	Sorting nexin 5
3170131	5.52	2810410P22Rik	75423	ADP-ribosylation factor-like 5A
6220128	5.51	Igfals	16005	Insulin-like growth factor binding protein, acid labile subunit
3170739	5.41	Ccl27	20301	Chemokine (C-C motif) ligand 27, transcript variant 2
5220097	5.02	Rarb	218772	Retinoic acid receptor beta
6940494	4.72	2810410P22Rik	75423	ADP-ribosylation factor-like 5A
270068	4.43	9630048M01Rik	320158	Zmat4 zinc finger, matrin type 4
7510072	4.38	Gstm2	14863	Glutathione S-transferase, mu 2
3850064	4.32	D15Ertd405e	380967	Transmembrane protein 106C (Tmem106c)
4120348	4.24	Krt42	68239	Keratin 42
1470332	4.18	9030425E11Rik	71566	RIKEN cdna 9030425E11 gene provided
70601	4.10	1600023A02Rik	67701	WAP four-disulfide core domain 2 (Wfdc2)
6130288	4.05	Mcm4	17217	Minichromosome maintenance deficient 4 homolog (S. Cerevisiae)
6040204	4.02	Vangl1	229658	Vang-like 1 (van gogh, Drosophila)
4830477	4.00	2810410P22Rik	75423	ADP-ribosylation factor-like 5A
1980682	3.99	Arv1	68865	ARV1 homolog (yeast)
290360	3.94	Slc44a1	100434	Solute carrier family 44, member 1
2100139	3.83	Bst2	69550	Bone marrow stromal cell antigen 2
2100176	3.82	Ly75	17076	Lymphocyte antigen 75
380332	3.82	Liph	239759	Lipase, member H
1240682	3.78	Zfp521	225207	Zinc finger protein 521
6560543	3.77	Lypla1	18777	Lysophospholipase 1
1070487	3.74	Nlrx1	270151	NLR family member X1
1580392	3.67	Pabpc1	18458	Poly A binding protein, cytoplasmic 1
5270382	3.64	Mcm4	17217	Minichromosome maintenance deficient 4 homolog (S. Cerevisiae)
5130221	3.64	Mid1ip1	68041	Mid1 interacting protein 1 (gastrulation specific G12-like (zebrafish)
510435	3.62	Zcchc3	67917	Zinc finger, CCHC domain containing 3

2690025	3.59	Gstm2	14863	Glutathione S-transferase, mu 2
7380164	3.58	Col2a1	12824	Collagen, type II, alpha 1
1470070	3.57	Ly6g6e	70274	Lymphocyte antigen 6 complex, locus G6E
2680746	3.56	3110050K21Rik	67302	Zinc finger CCCH type containing 13
4260762	3.46	AI661438	104871	Spermatogenesis associated 7 (Spata7)
3060382	3.42	Odz4	23966	Odd Oz/ten-m homolog 4 (Drosophila)
1230240	3.38	Igfbp2	16008	Insulin-like growth factor binding protein 2
5570093	3.36	Arbp	11837	Acidic ribosomal phosphoprotein P0
7380167	3.36	BC003993	80744	Cdna sequence BC003993
2480471	3.31	Eif4e	13684	Eukaryotic translation initiation factor 4E
6840458	3.31	Csde1	229663	Cold shock domain containing E1, RNA binding
6040292	3.31	Tgfb1i4	97848	TSC22 domain family, member 1
2970500	3.29	Serpinb6c	97848	Serine (or cysteine) peptidase inhibitor, clade B, member 6c
7330551	3.29	Sall4	99377	Sal-like 4 (Drosophila)
650168	3.29	Ivns1abp	117198	Influenza virus NS1A binding protein, transcript variant 1
730025	3.23	Gstm2	14863	Glutathione S-transferase, mu 2
2230379	3.23	Liph	239759	Lipase, member H
4260307	3.19	Sfrs16	53609	CLK4-associating serine/arginine rich protein
6380113	3.17	Rpap1	68925	RNA polymerase II associated protein 1
4280246	3.17	4930504E06Rik	75007	RIKEN cdna 4930504E06 gene
630427	3.16	Sox2	20674	SRY-box containing gene 2
7200068	3.11	Mkks	59030	Mckusick-Kaufman syndrome protein
6420372	3.11	BC013481	245945	Cdna sequence BC013481
6550133	3.10	Eif4b	75705	Eif4b eukaryotic translation initiation factor 4B
4560278	3.10	AA536743	100532	Rell1 RELT-like 1
6760228	3.07	Elmo1	140580	Engulfment and cell motility 1, ced-12 homolog (C. Elegans), transcript variant 2
3850747	3.07	Ildr1	106347	Immunoglobulin-like domain containing receptor 1
6480053	3.06	Eva1	14012	Epithelial V-like antigen 1
4070037	3.06	Hdlbp	110611	High density lipoprotein (HDL) binding protein
4810725	3.04	Nr5a2	26424	Nuclear receptor subfamily 5, group A,member 2
4260747	3.03	Ube1x	22201	Ubiquitin-activating enzyme E1
3130424	3.02	Tex13	83555	Testis expressed gene 13
1240424	3.01	Nupr1	56312	Nuclear protein 1

Table 3A: Transcripts that were higher by 3-fold or more in WT ES cells compared to RARγ KO ES cells treated with RA for 8 hrs (a total of 56 transcripts)

Probe ID	Fold decrease [RARγKO-8] vs [WT-8]	Symbol	Entrez Gene ID	Definition
7610097	9.58	Spink3	20730	Serine peptidase inhibitor, Kazal type 3
5290711	9.57	Car2	12349	Carbonic anhydrase 2
4070142	8.42	Gadd45g	23882	Growth arrest and DNA-damage-inducible 45 gamma
1500286	8.41	Car4	12351	Carbonic anhydrase 4
5130528	7.92	MGC117846	626316	Gm13051
990326	7.34	2810422B04Rik	69956	Pentatricopeptide repeat domain 3
1450408	6.55	6330407J23Rik	67412	RIKEN cdna 6330407J23 gene
7320056	6.42	Bat5	53772	HLA-B associated transcript 5
4890402	6.39	Tesk1	21754	Testis specific protein kinase 1
3060470	6.12	Peg10	170676	Paternally expressed 10 transcript variant 1
870484	5.84	4930455C21Rik	76916	RIKEN cdna 4930455C21 gene (4930455C21Rik)
1820746	5.58	Pitx2	18741	Paired-like homeodomain transcription factor 2, transcript variant 3
4900743	5.40	Atp10d	231287	Atpase, Class V, type 10D
6220639	5.19	Hoxb1	15407	Homeobox B1
7320338	5.17	Pitx2	18741	Paired-like homeodomain transcription factor 2 (Pitx2), transcript variant 3
4570451	4.90	Cdkn1c	12577	Cyclin-dependent kinase inhibitor 1C (P57)
4780102	4.83	1700029P11Rik	66346	RIKEN cdna 1700029P11 gene
360025	4.48	Hoxb2	103889	Homeobox B2
270274	4.28	Rpo1-4	20019	Polymerase (RNA) I polypeptide A
3850326	4.22	Itgb4	192897	Integrin beta 4
2850543	4.12	1700029P11Rik	66346	RIKEN cdna 1700029P11 gene (1700029P11Rik)
5130136	4.00	Hoxb5	15413	Homeobox B5
4480180	3.96	Phlda1	21664	Pleckstrin homology-like domain, family A, member 1
4540564	3.69	Dok2	13449	Docking protein 2
6940278	3.61	Bmp1	12153	Bone morphogenetic protein 1
6940544	3.59	En2	13799	Engrailed 2
1710193	3.56	Gja1	14609	Gap junction membrane channel protein alpha 1
2630021	3.53	Efha1	68514	EF hand domain family A1
6040066	3.52	Cdx2	12591	Caudal type Homeobox 2
1010050	3.50	Lmo4	16911	LIM domain only 4
3460189	3.48	Sox17	20671	SRY-box containing gene 17
4490253	3.47	AV071179	100876	Expressed sequence AV071179
5270279	3.42	Alox5ap	11690	Arachidonate 5-lipoxygenase activating protein (Alox5ap), mrna.
3170348	3.39	Hoxb1	15407	Homeobox B1
3360553	3.29	Ccrn4l	12457	CCR4 carbon catabolite repression 4-like (S. Cerevisiae).
1980411	3.29	Arrdc3	105171	Arrestin domain containing 3

5720328	3.27	Nrip1	268903	Nuclear receptor interacting protein 1
5670554	3.26	2300002G24Rik	74175	Cysteine-rich C-terminal 1
460682	3.25	2200001I15Rik	69134	RIKEN cdna 2200001I15 gene
4900592	3.22	Hrmt1l1	15468	Protein arginine N-methyltransferase 2
3990563	3.19	BC036718	213484	Nudt18 nudix (nucleoside diphosphate linked moiety X)-type motif 18
5670246	3.16	2900011O08Rik	67254	2900011O08Rik RIKEN cdna 2900011O08 gen
4050400	3.16	Zyx	22793	Zyxin
50079	3.14	Hist1h1c	50708	Histone cluster 1, H1c
5720112	3.14	Hoxa7	15404	Homeobox A7
1780619	3.13	Rab32	67844	RAB32, member RAS oncogene family (Rab32)
4610433	3.12	Prg	19073	Serglycinp
1030497	3.11	Irak3	73914	Interleukin-1 receptor-associated kinase 3
2480059	3.11	Anxa5	11747	Annexin A5
3140274	3.08	Dcxr	67880	Dicarbonyl L-xylulose reductase
4880187	3.05	Erdr1	170942	Erythroid differentiation regulator 1
4560280	3.04	2600001B17Rik	268490	LSM12 homolog (S. Cerevisiae)
5860343	3.03	Stra8	20899	Stimulated by retinoic acid gene 8
6520022	3.02	1300013J15Rik	67473	RIKEN cdna 1300013J15 gene (1300013J15Rik)
1240095	3.02	Snx24	69226	Sorting nexing 24
1190431	3.01	Lama1	16772	Laminin, alpha 1

Table 3B: Transcripts that were higher by 3-fold or more in RARγ KO ES cells compared to WT ES cells treated with RA for 8 hrs

Probe ID	Fold increase [RARγKO-8] vs [WT-8]	Symbol	Entrez Gene ID	Definition
3990243	36.87	Mcm6	17219	Minichromosome maintenance deficient 6 (MIS5 homolog, S. Pombe) (S. Cerevisiae)
7200376	30.38	Barx1	12022	Barh-like homeobox 1
2940164	9.82	Rbm13	67920	RNA binding motif protein 13
6900546	8.82	Ccl25	20300	Chemokine (C-C motif) ligand 25
7100301	6.99	2810417H13Rik	68026	RIKEN cdna 2810417H13 gene
6220128	6.20	Igfals	16005	Insulin-like growth factor binding protein, acid labile subunit
2100333	6.01	Lrrc57	66606	Leucine rich repeat containing 57
7380142	5.85	Snx5	69178	Sorting nexin 5
5570093	5.78	Arbp	11837	Acidic ribosomal phosphoprotein P0
5290360	5.62	Picalm	233489	Picalm phosphatidylinositol binding clathrin assembly protein
4120348	5.51	Krt42	68239	Keratin 42
1240424	5.28	Nupr1	56312	Nuclear protein 1
3170131	5.23	2810410P22Rik	75423	ADP-ribosylation factor-like 5A
5130221	5.15	Mid1ip1	68041	Mid1 interacting protein 1 (gastrulation specific G12-like (zebrafish)
990672	4.98	Fbxl3a	50789	F-box and leucine-rich repeat protein 3
6940494	4.86	2810410P22Rik	75423	ADP-ribosylation factor-like 5A
7330551	4.75	Sall4	99377	Sal-like 4 (Drosophila)
2690025	4.36	Gstm2	14863	Glutathione S-transferase, mu 2
7510072	4.36	Gstm2	14863	Glutathione S-transferase, mu 2
6060730	4.33	Lars2	102436	Leucyl-trna synthetase, mitochondrial
1990520	4.14	Epm2aip1	77781	EPM2A (laforin) interacting protein 1
290360	4.08	Slc44a1	100434	Solute carrier family 44, member 1
2900373	4.06	1190002H23Rik	66214	RIKEN cdna 1190002H23 gene
3170739	4.03	Ccl27	20301	Chemokine (C-C motif) ligand 27 transcript variant 2
1470035	3.99	Myo10	17909	Myosin X
6040292	3.92	Tgfb1i4	21807	TSC22 domain family, member 1
70601	3.91	1600023A02Rik	67701	WAP four-disulfide core domain 2 (Wfdc2).
6560543	3.89	Lypla1	18777	Lysophospholipase 1
2100139	3.89	Bst2	69550	Bone marrow stromal cell antigen 2
3780711	3.81	Tcfap2c	21420	Transcription factor AP-2, gamma
3850064	3.71	D15Ertd405e	380967	Transmembrane protein 106C (Tmem106c)
6380113	3.67	Rpap1	68925	RNA polymerase II associated protein 1
510435	3.57	Zcchc3	67917	Zinc finger, CCHC domain containing 3
3290402	3.57	Pgc	109820	Progastricsin (pepsinogen C)
7050487	3.56	Cd63	12512	CD63 antigen
5220279	3.48	Mt1	17748	Metallothionein 1
4260762	3.38	AI661438	104871	Spermatogenesis associated 7 (Spata7)
1580707	3.38	Snx5	69178	Sorting nexin 5
6660553	3.37	2610101N10Rik	67958	RIKEN cdna 2610101N10 gene
6960376	3.36	2410012C07Rik	76484	Kinase non-catalytic C-lobe domain (KIND)

				containing 1
7160047	3.36	AA467197	433470	Expressed sequence AA467197
1070487	3.35	Nlrx1	270151	NLR family member X1
540300	3.31	1810008K03Rik	69065	Chac, cation transport regulator-like 1 (E. Coli) (Chac1)
6420551	3.28	Parp1	11545	Poly (ADP-ribose) polymerase family,member 1
2370053	3.27	2410146L05Rik	67968	RIKEN cdna 2410146L05 gene
2100176	3.26	Ly75	17076	Lymphocyte antigen 75
5080326	3.25	S100a6	20200	S100 calcium binding protein A6 (calcyclin)
2480471	3.21	Eif4e	13684	Eukaryotic translation initiation factor 4E
4920736	3.14	Anp32a	11737	Acidic (leucine-rich) nuclear phosphoprotein 32 family, member A
6270243	3.12	BC013481	245945	Cdna sequence BC013481
4640768	3.11	BC003993	80744	Cdna sequence BC003993
6270131	3.09	2310009N05Rik	66943	PQ loop repeat containing 1 (Pqlc1)
1340762	3.09	Tiam2	24001	T-cell lymphoma invasion and metastasis 2
2760470	3.08	2410116G06Rik	68236	RIKEN cdna 2410116G06 gene
4040386	3.06	Hspb6	243912	Heat shock protein, alpha-crystallin-related,B6
730025	3.06	Gstm2	14863	Glutathione S-transferase, mu 2
2850082	3.03	1200003I07Rik	66869	RIKEN cdna 1200003I07 gene, transcript variant 3
780376	3.01	Manba	110173	Mannosidase, beta A, lysosomal
2350484	3.00	Eef2	13629	Eukaryotic translation elongation factor 2

Table 4A: Transcripts that were higher by 3-fold or more in WT ES cells compared to RARγ KO ES cells treated with RA for 24 hrs

Probe ID	Fold decrease [RARγKO-24] vs [WT-24]	Symbol	Entrez Gene ID	Definition
6960730	37.44	Eif2s3y	26908	Eukaryotic translation initiation factor 2, subunit 3, structural gene Y-linked
6220639	17.53	Hoxb1	15407	Homeobox B1
360025	14.50	Hoxb2	103889	Homeobox B2
3610347	13.40	Fbp2	14120	Fructose bisphosphatase 2
3170348	11.09	Hoxb1	15407	Homeobox B1
6770519	10.50	Hoxa4	15401	Homeobox A4
2480129	9.62	Pmp22	18858	Peripheral myelin protein 22
630470	9.28	Mrpl35	66223	Mitochondrial ribosomal protein L35
3610202	9.21	Bing4	57315	WD repeat domain 46 (Wdr46)
3060470	9.19	Peg10	170676	Paternally expressed 10, transcript variant 1
1450408	8.00	6330407J23Rik	67412	RIKEN cdna 6330407J23 gene
4760255	7.57	A130072J07	240832	Torsin A interacting protein 2 (Tor1aip2)
7320343	7.05	Bing4	57315	WD repeat domain 46 (Wdr46)
5290521	6.70	Pdgfra	18595	Platelet derived growth factor receptor, alpha polypeptide.
5130528	6.65	MGC117846	626316	Predicted gene
10703	6.48	Gm397	245109	Gene model 397
2260551	6.22	Col4a2	12827	Procollagen, type IV, alpha 2
1570220	6.11	Hoxb6	15414	Homeobox B6
990326	5.74	2810422B04Rik	69956	Pentatricopeptide repeat domain 3
650402	5.74	Hoxa1	15394	Homeobox A1
3130661	5.52	Fgfbp3	72514	Fibroblast growth factor binding protein 3
7320338	5.49	Pitx2	18741	Paired-like homeodomain transcription factor 2, transcript variant 3
1300475	5.34	Stra6	20897	Stimulated by retinoic acid gene 6
3450719	5.18	Mbnl2	105559	Muscleblind-like 2 (Mbnl2), transcript variant 2
270274	5.11	Rpo1-4	20019	Polymerase (RNA) I polypeptide A
4900743	5.04	Atp10d	231287	Atpase, Class V, type 10D
7610239	4.98	2510009E07Rik	72190	RIKEN cdna 2510009E07 gene
2710142	4.87	Mbnl2	105559	Muscleblind-like 2,transcript variant 1
380639	4.79	Sertad4	214791	SERTA domain containing 4
1940347	4.75	Dab2	13132	Disabled homolog 2 (Drosophila), transcript variant 2
1050609	4.70	Dab2	13132	Disabled homolog 2 (Drosophila) transcript variant 2
6180348	4.58	Crabp2	12904	Cellular retinoic acid binding protein II
3460189	4.54	Sox17	20671	SRY-box containing gene 17

2940446	4.16	Sox17	20671	SRY-box containing gene 17
5670739	3.99	Msx1	17701	Homeobox, msh-like 1
4070142	3.91	Gadd45g	23882	Growth arrest and DNA-damage-inducible 45 gamma
3940242	3.87	AA175286	209086	Sterile alpha motif domain containing 9-like
10435	3.75	Rnf20	109331	Ring finger protein 20
4880187	3.75	Erdr1	170942	Erythroid differentiation regulator
4480180	3.67	Phlda1	21664	Pleckstrin homology-like domain, family A, member 1
6520722	3.65	Pbx1	18514	Pre B-cell leukemia transcription factor 1
3870056	3.58	Cyp26a1	13082	Cytochrome P450, family 26, subfamily a, polypeptide 1
1190445	3.57	Arg1	11846	Arginase 1, liver
2140678	3.56	Tmem150	232086	Transmembrane protein 150
6040445	3.53	Tcte3	21647	T-complex-associated testis expressed 3 , transcript variant 2,
5720112	3.51	Hoxa7	15404	Homeobox A7
1440543	3.48	H19	14955	H19 fetal liver mrna on chromosome 7
160079	3.47	LOC626391	626391	Similar to Zinc finger protein 124 (HZF-16)
6330195	3.44	Camk2n1	66259	Calcium/calmodulin-dependent protein kinase II inhibitor 1
2600286	3.43	Fgf10	14165	Fibroblast growth factor 10
7550451	3.42	Hoxa2	15399	Homeobox A2
3400368	3.36	Hoxc9	15427	Homeobox C9
4860537	3.33	Pknox2	208076	Pbx/knotted 1 homeobox 2 transcript variant 2
5130494	3.29	Cald1	109624	Caldesmon 1
1410348	3.26	F2rl1	14063	Coagulation factor II (thrombin) receptor-like 1
10176	3.21	Dusp4	60587	Dual specificity phosphatase 4
2970736	3.21	Sox7	20680	SRY-box containing gene 7
3360553	3.20	Ccrn4l	12457	CCR4 carbon catabolite repression 4-like (S. Cerevisiae)
6550082	3.19	Lamb1-1	16777	Laminin B1
2760537	3.18	Zic1	22771	Zinc finger protein of the cerebellum 1
5220259	3.18	Hoxa2	15399	Homeobox A2
1170255	3.16	A230098A12Rik	235472	Protogenin homolog (Gallus gallus)
4570451	3.16	Cdkn1c	12577	Cyclin-dependent kinase inhibitor 1C (P57)
3850326	3.15	Itgb4	192897	Integrin beta 4
4010224	3.14	Egfr	13649	Epidermal growth factor receptor
940598	3.13	Rex2	19715	Reduced expression 2
7320593	3.13	Cugbp2	14007	CUGBP, Elav-like family member 2
5720328	3.09	Nrip1	268903	Nuclear receptor interacting protein 1
7000465	3.07	Gpr177	68151	G protein-coupled receptor 177
870445	3.04	Lamc2	16782	Laminin, gamma 2
1340328	3.03	LOC381813	381813	Protein arginine N-methyltransferase 8 (Prmt8)

Table 4B: Transcripts that were higher by 3-fold or more in RARγ KO ES cells compared to WT ES cells treated with RA for 24 hrs

Probe ID	Fold increase [RARγKO-24] vs. [WT-24]	Symbol	Entrez Gene ID	Definition
3990243	42.56	Mcm6	17219	Minichromosome maintenance deficient 6 (MIS5 homolog, S. Pombe) (S. Cerevisiae)
4880603	27.53	Barx1	12022	Barh-like homeobox 1
7200376	25.06	Barx1	12022	Barh-like homeobox 1
520427	21.91	Plk1	18817	Polo-like kinase 1
2940164	13.19	Rbm13	67920	RNA binding motif protein 13
6900546	11.17	Ccl25	20300	Chemokine (C-C motif) ligand 25
7100301	6.77	2810417H13Rik	68026	RIKEN cdna 2810417H13 gene
7380142	6.08	Snx5	69178	Sorting nexin 5
1300202	5.87	Eprs	107508	Glutamyl-prolyl-trna synthetase
2100333	5.80	Lrrc57	66606	Leucine rich repeat containing 57
5290360	5.73	Picalm	233489	Picalm phosphatidylinositol binding clathrin assembly protein
3170131	5.55	2810410P22Rik	75423	ADP-ribosylation factor-like 5A
990672	5.51	Fbxl3a	50789	F-box and leucine-rich repeat protein 3
1410142	5.29	BC038156	270135	BC038156 cdna sequence
6060730	5.18	Lars2	102436	Leucyl-trna synthetase, mitochondrial
3170739	5.08	Ccl27	20301	Chemokine (C-C motif) ligand 27, transcript variant 2
6940494	4.90	2810410P22Rik	75423	ADP-ribosylation factor-like 5A
1990520	4.75	Epm2aip1	77781	EPM2A (laforin) interacting protein 1
2900373	4.57	1190002H23Rik	66214	RIKEN cdna 1190002H23 gene
630427	4.55	Sox2	20674	SRY-box containing gene 2
7330551	4.44	Sall4	99377	Sal-like 4 (Drosophila)
5570093	4.27	Arbp	11837	Acidic ribosomal phosphoprotein P0
1980682	3.88	Arv1	68865	ARV1 homolog (yeast)
5870021	3.87	Xlr4a	434794	X-linked lymphocyte-regulated 4A
3520408	3.81	Mobp	17433	Myelin-associated oligodendrocytic basic protein
70601	3.78	1600023A02Rik	67701	WAP four-disulfide core domain 2 (Wfdc2)
510435	3.70	Zcchc3	67917	Zinc finger, CCHC domain containing 3
1070324	3.61	E130309F12Rik	272031	RIKEN cdna E130309F12 gene
7510072	3.59	Gstm2	14863	Glutathione S-transferase, mu 2
1430576	3.59	2610206B13Rik	72486	RIKEN cdna 2610206B13 gene
2690360	3.56	Mobp	17433	Myelin-associated oligodendrocytic basic protein, transcript variant 3
6370184	3.51	Ebaf	320202	Left-right determination factor 2 (Lefty2)
1850241	3.45	Cdyl2	75796	Chromodomain protein, Y chromosome-like 2
1230240	3.43	Igfbp2	16008	Insulin-like growth factor binding protein 2
2370053	3.42	2410146L05Rik	67968	RIKEN cdna 2410146L05 gene
6840112	3.33	Uap1	107652	UDP-N-acetylglucosamine pyrophosphorylase 1
6130288	3.31	Mcm4	17217	Minichromosome maintenance deficient 4 homolog (S. Cerevisiae)

7200068	3.31	Mkks	59030	Mckusick-Kaufman syndrome protein
3850064	3.30	D15Ertd405e	380967	Transmembrane protein 106C (Tmem106c)
1580392	3.24	Pabpc1	18458	Poly A binding protein, cytoplasmic 1
1340762	3.23	Tiam2	24001	T-cell lymphoma invasion and metastasis 2
1170228	3.19	Tdh	58865	L-threonine dehydrogenase
1780307	3.19	Ccl25	20300	Chemokine (C-C motif) ligand 25
7210367	3.17	Otx2	18424	Orthodenticle homolog 2 (Drosophila)
6770603	3.15	Col2a1	12824	Collagen, type II, alpha 1
4260762	3.11	AI661438	104871	Spermatogenesis associated 7 (Spata7)
4830477	3.09	2810410P22Rik	75423	ADP-ribosylation factor-like 5A

Table 5: Trancripts that increased by 2.5 fold or more in WT ES cells treated with RA for 8 h compared to untreated WT ES cells

Probe ID	Fold increase [WT-8] vs [WT-0]	Symbol	Entrez Gene ID	Definition
7100291	8.11	Hoxa5	15402	Homeobox A5
5860343	7.58	Stra8	20899	Stimulated by retinoic acid gene 8
650402	6.42	Hoxa1	15394	Homeobox A1
5130136	6.12	Hoxb5	15413	Homeobox B5
1980156	5.07	H2-Bl	14963	Histocompatibility 2, blastocyst
6960564	4.63	Hoxb4	15412	Homeobox B4
360025	4.35	Hoxb2	103889	Homeobox B2
2650131	4.16	Rarb	218772	Retinoic acid receptor, beta (Rarb)
6220639	3.95	Hoxb1	15407	Homeobox B1 (Hoxb1)
130672	3.83	Dleu7	239133	Deleted in lymphocytic leukemia 7
6770519	3.66	Hoxa4	15401	Homeobox A4
6400367	3.65	Cdx1	12590	Caudal type homeobox 1
4730685	3.57	Pmp22	18858	Peripheral myelin protein 22
780445	3.54	Tle6	114606	Transducin-like enhancer of split 6, homolog of Drosophila E(spl)
3360161	3.31	Aqp3	11828	Aquaporin 3
2320634	3.25	Csn3	12994	Casein kappa
5220097	3.10	Rarb	218772	Retinoic acid receptor, beta
4180471	3.05	Nt5e	23959	5' nucleotidase, ecto (Nt5e)
6860609	3.02	Rbp1	19659	Cellular retinol-binding protein I
3610619	2.98	Nt5e	23959	5' nucleotidase, ecto
7200100	2.97	H2-T23	15040	Histocompatibility 2, T region locus 23
2260746	2.96	BC024955	233552	Glycerophosphodiester phosphodiesterase domain containing 5
6060307	2.82	Nphp4	260305	Nphp4 nephronophthisis 4 (juvenile) homolog (human)
3170348	2.78	Hoxb1	15407	Homeobox B1
130750	2.67	BC023818	387314	Transmembrane and tetratricopeptide repeat containing 1 (Tmtc1)
6330195	2.66	Camk2n1	66259	Calcium/calmodulin-dependent protein kinase II inhibitor 1
2470441	2.64	Hoxb7	15415	Homeobox B7
380639	2.62	Sertad4	214791	SERTA domain containing 4
3290500	2.58	Cdx1	12590	Caudal type Homeobox 1

Table 6A: Transcripts that increased by 2.5 fold or more in WT ES cells treated with RA for 24 h compared to untreated WT ES cells

Probe ID	Fold increase [WT-24] vs. [WT-0]	Symbol	Entrez Gene ID	Definition
360025	21.63	Hoxb2	103889	Homeobox B2
7100291	20.47	Hoxa5	15402	Homeobox A5
5130136	19.50	Hoxb5	15413	Homeobox B5
6220639	16.52	Hoxb1	15407	Homeobox B1
4730685	12.85	Pmp22	18858	Peripheral myelin protein 22
6860609	10.90	Rbp1	19659	Cellular retinol-binding protein I
6960564	10.55	Hoxb4	15412	Homeobox B4
3170348	10.54	Hoxb1	15407	Homeobox B1
650402	10.53	Hoxa1	15394	Homeobox A1
5860343	10.52	Stra8	20899	Stimulated by retinoic acid gene 8
6770519	10.36	Hoxa4	15401	Homeobox A4
3890431	7.86	Crygc	12966	Crystallin, gamma C, transcript variant 1
2650131	7.40	Rarb	218772	Retinoic acid receptor beta
2320634	7.00	Csn3	12994	Casein kappa
1820746	6.63	Pitx2	18741	Paired-like homeodomain transcription factor 2 transcript variant 3
2480129	6.57	Pmp22	18858	Peripheral myelin protein 22
7320338	6.29	Pitx2	18741	Paired-like homeodomain transcription factor 2 transcript variant 3
2470441	6.20	Hoxb7	15415	Homeobox B7
6400367	6.00	Cdx1	12590	Caudal type Homeobox 1
1300475	5.96	Stra6	20897	Stimulated by retinoic acid gene 6
3610619	5.73	Nt5e	23959	5' nucleotidase, ecto
1980156	5.63	H2-Bl	14963	Histocompatibility 2, blastocyst
6350196	5.63	Mrg1	17536	Myeloid ecotropic viral integration site-related gene
5220097	5.56	Rarb	218772	Retinoic acid receptor, beta
7510341	5.55	Ap3b2	11775	Adaptor-related protein complex 3, beta 2 subunit
4250246	4.96	Cyp1b1	13078	Cytochrome P450, family 1, subfamily B, polypeptide 1
4180471	4.91	Nt5e	23959	5' nucleotidase, ecto
7560647	4.78	Meis1	17268	Meis homeobox 1
4230730	4.58	Zadh2	225791	Zinc binding alcohol dehydrogenase, domain containing 2
5720112	4.57	Hoxa7	15404	Homeobox A7
4860537	4.56	Pknox2	208076	Pbx/knotted 1 homeobox 2 transcript variant 2
4890747	4.49	Rgma	244058	RGM domain family, member A
3130661	4.42	Fgfbp3	72514	Fibroblast growth factor binding protein 3
6180348	4.37	Crabp2	12904	Cellular retinoic acid binding protein II
7610239	4.34	2510009E07Rik	72190	RIKEN cdna 2510009E07 gene
5700066	4.26	4930422J18Rik	74646	Spla/ryanodine receptor domain and SOCS box containing 1 (Spsb1)

7550451	4.13	Hoxa2	15399	Homeobox A2
130672	4.05	Dleu7	239133	Deleted in lymphocytic leukemia, 7
380639	4.05	Sertad4	214791	SERTA domain containing 4
3290500	3.89	Cdx1	12590	Caudal type Homeobox 1
3870056	3.89	Cyp26a1	13082	Cytochrome P450, family 26, subfamily a, polypeptide
2060546	3.82	Tnfrsf19	29820	Tumor necrosis factor receptor superfamily, member 19
6520722	3.82	Pbx1	18514	Pre B-cell leukemia transcription factor 1
3440767	3.73	9230117N10Rik	77125	Interleukin 33 (Il33)
4810187	3.70	Leftb	69051	Pyrroline-5-carboxylate reductase family, member 2
5220259	3.65	Hoxa2	15399	Homeobox A2
5670739	3.63	Msx1	17701	Homeobox, msh-like 1
6330195	3.61	Camk2n1	66259	Calcium/calmodulin-dependent protein kinase II inhibitor 1
6350678	3.60	Gata6	14465	GATA binding protein 6
2490575	3.58	Serpinf1	20317	Serine (or cysteine) peptidase inhibitor, clade F, member 1
2600026	3.55	Rec8L1	56739	REC8 homolog (yeast)
7000187	3.51	Tgm2	21817	Transglutaminase 2, C polypeptide
1170255	3.42	A230098A12Rik	235472	Prtg protogenin homolog (Gallus gallus)
430392	3.42	Sp8	320145	Trans-acting transcription factor 8
1400152	3.39	Efnb1	13641	Ephrin B1
7200100	3.37	H2-T23	15040	Histocompatibility 2, T region locus 23
6980487	3.36	Clgn	12745	Calmegin
2030440	3.20	Chrna5	110835	Cholinergic receptor, nicotinic, alpha polypeptide 5
430670	3.20	Foxa1	15375	Forkhead box A1
990438	3.19	Cotl1	72042	Coactosin-like 1 (Dictyostelium)
1430368	3.18	St6gal1	20440	Beta galactoside alpha 2,6 sialyltransferase 1
2450100	3.12	Punc	19289	Immunoglobulin superfamily, DCC subclass, member 3
780750	3.08	Hic1	15248	Hypermethylated in cancer 1
6510025	3.07	Ndp52	76815	Nuclear domain 10 protein 52
7550121	3.05	Tes	21753	Testis derived transcript (Tes), transcript variant 1
5310091	3.04	Add3	27360	Adducin 3 (gamma)
3610239	2.97	2810003C17Rik	108897	Aif1l allograft inflammatory Factor 1-like
1690687	2.89	Rnf103	22644	Ring finger protein 103
1980138	2.88	Mdk	17242	Midkine
3450040	2.87	Add3	27360	Adducin 3 (gamma)
2850020	2.84	Dlk1	13386	Delta-like 1 homolog
1770592	2.78	1200013B22Rik	74137	NUAK family, SNF1-like kinase, 2
780445	2.77	Tle6	114606	Transducin-like enhancer of split 6, homolog of Drosophila E(spl)
1820215	2.76	BC039093	230761	Zfp362 zinc finger protein 362

4830010	2.76	Oasl2	23962	2'-5' oligoadenylate synthetase-like 2
6770356	2.74	Mest	17294	Mesoderm specific transcript.
7400603	2.74	2810004A10Rik	171463	Il17rd interleukin 17 receptor D
6980048	2.74	Olig3	94222	Oligodendrocyte transcription factor 3
6130703	2.71	Hoxa1	15394	Homeobox A1
1580088	2.68	Ccnd2	12444	Cyclin D2
2260746	2.67	BC024955	233552	Glycerophosphodiester phosphodiesterase domain containing 5
670133	2.66	Hmgn3	94353	High mobility group nucleosomal binding domain 3, transcript variant 2
730692	2.62	Eml1	68519	Echinoderm microtubule associated protein like 1
6420750	2.60	Sall2	50524	Sal-like 2
50025	2.59	Raet1b	19369	Retinoic acid early transcript beta
7000465	2.57	Gpr177	68151	G protein-coupled receptor 177
2690743	2.56	Shd	20420	Src homology 2 domain-containing transforming protein D
1470079	2.53	2610041P08Rik	78317	Ccdc88b coiled-coil domain containing 88B
6860309	2.53	B230104P22Rik	77976	Nuak1 NUAK family, SNF1-like kinase, 1
4250121	2.52	Hmgn3	94353	High mobility group nucleosomal binding domain 3 transcript variant 2

Table 6B: Transcripts that decreased by 2.5 fold or more in WT ES cells treated with RA for 24 h compared to untreated WT ES cells

Probe ID	Fold decrease [WT-24] vs [WT-0]	Symbol	Entrez GeneID	Definition
7210367	8.09	Otx2	18424	Orthodenticle homolog 2
1170228	5.24	Tdh	58865	L-threonine dehydrogenase
3060746	5.24	D230005D02Rik	239188	RIKEN cdna D230005D02 gene
6330048	4.22	8430410A17Rik	232210	RIKEN cdna 8430410A17 gene
5820008	4.06	C730015A04Rik	277978	Exocyst complex component 3-like
5340731	4.00	Tcfcp2l3	252973	Grainyhead-like 2 (Drosophila)
5340747	3.64	Gm525	217071	Gene model 525
4250239	3.56	Lrrc34	71827	Leucine rich repeat containing 34
1990484	3.49	Tcl1	21432	T-cell lymphoma breakpoint 1
2070594	3.39	Dnajc6	72685	Dnaj (Hsp40) homolog, subfamily C, member 6
5700044	3.29	Bmp4	12159	Bone morphogenetic protein 4
2490142	3.19	Ddx58	230073	DEAD box protein 58
6940537	3.19	Dnajc6	72685	Dnaj (Hsp40) homolog, subfamily C, member 6
510474	3.11	Lgals3	16854	Lectin, galactose binding, soluble 3
6250180	3.11	Cyp2s1	74134	Cytochrome P450, family 2, subfamily s, polypeptide 1
830521	3.08	Zfp296	63872	Zinc finger protein 296
3370221	3.07	BC028528	229600	Cdna sequence BC028528
1660221	3.01	Chrna9	231252	Cholinergic receptor, nicotinic, alpha polypeptide 9
270068	2.99	9630048M01Rik	320158	Zmat4 zinc finger, matrin type 4
3060577	2.96	2410116G06Rik	68236	RIKEN cdna 2410116G06 gene
6450309	2.93	Slc27a2	26458	Solute carrier family 27 (fatty acid transporter), member 2
6350349	2.93	Slc7a3	11989	Solute carrier family 7 (cationic amino acid transporter, y+ system), member 3
1780341	2.90	Krt1-17	16667	Keratin 17
4050064	2.85	Ngfr	18053	Nerve growth factor receptor (TNFR superfamily, member 16)
2900274	2.80	1700007J06Rik	71827	Leucine rich repeat containing 34
2320554	2.80	Slc28a1	434203	Solute carrier family 28 (sodium-coupled nucleoside transporter), member 1
3440692	2.78	Spry4	24066	Sprouty homolog 4 (Drosophila)
5870136	2.77	Pla2g10	26565	Phospholipase A2, group X
2680438	2.77	Tcl1	21432	T-cell lymphoma breakpoint 1
1110372	2.73	Zfp42	22702	Zinc finger protein 42
2760470	2.72	2410116G06Rik	68236	RIKEN cdna 2410116G06 gene
4810725	2.68	Nr5a2	26424	Nuclear receptor subfamily 5, group A, member 2
450563	2.65	Sept	54204	Septin 1
6270739	2.59	Gcnt2	14538	Glucosaminyl (N-acetyl) transferase 2, I-branching enzyme, transcript variant 1
3360224	2.58	Fgf17	14171	Fibroblast growth factor 17

380215	2.58	Tor3a	30935	Torsin family 3, member A
1820433	2.56	5730593N15Rik	77583	Notum pectinacetylesterase homolog (Drosophila)
5670154	2.55	Zfp296	63872	Zinc finger protein 296
2690603	2.55	Zfp459	328274	Zinc finger protein 459
6040364	2.52	Dtr	15200	Heparin-binding EGF-like growth factor

Table 7A: Transcripts that were 2.5-fold or more higher in RARγ KO ES cells treated with RA for 24 h compared to untreated RARγ KO ES cells

Probe ID	Fold increase RARγKO-24] vs [RARγKO-0]	Symbol	Entrez Gene ID	Definition
5860343	8.50	Stra8	20899	Stimulated by retinoic acid gene 8
1820746	7.82	Pitx2	18741	Paired-like homeodomain transcription factor 2 transcript variant 3
6400367	5.55	Cdx1	12590	Caudal type Homeobox 1
5130136	4.46	Hoxb5	15413	Homeobox B5
3890431	4.38	Crygc	12966	Crystallin, gamma C transcript variant 1
6860609	4.37	Rbp1	19659	Cellular retinol-binding protein I
650402	4.33	Hoxa1	15394	Homeobox A1
4810187	4.32	Leftb	69051	Pyrroline-5-carboxylate reductase family, member 2
3060546	4.04	Dpp4	13482	Dipeptidylpeptidase 4
3290500	4.04	Cdx1	12590	Caudal type Homeobox 1
7100291	4.03	Hoxa5	15402	Homeobox A5
130672	3.88	Dleu7	239133	Deleted in lymphocytic leukemia 7
4250059	3.51	Notch4	18132	Notch gene homolog 4 (Drosophila)
2470441	3.34	Hoxb7	15415	Homeobox B7
7320338	3.22	Pitx2	18741	Paired-like homeodomain transcription factor 2 transcript variant 3
3360161	2.96	Aqp3	11828	Aquaporin 3
6980487	2.81	Clgn	12745	Calmegin
4900053	2.76	Ier5l	72500	Immediate early response 5-like
60136	2.72	Foxn4	116810	Forkhead box N4
3390326	2.64	BC046404	192976	Cdna sequence BC046404
3420156	2.63	Col9a2	12840	Procollagen, type IX, alpha 2
6510025	2.60	Ndp52	76815	Nuclear domain 10 protein 52
1570291	2.58	BC046404	192976	Cdna sequence BC046404

Table 7B: Transcripts that decreased by 2.5-fold or more in RARγ KO ES cells treated with RA for 24 hrs compared to untreated RARγ KO ES cells

Probe ID	Fold decrease [RARγKO-24] vs. [RARγKO-0]	Symbol	Entrez Gene ID	Definition
3360224	3.27	Fgf17	14171	Fibroblast growth factor 17
2490142	2.88	Ddx58	230073	DEAD box protein 58
1470070	2.85	Ly6g6e	70274	Lymphocyte antigen 6 complex, locus G6E
6330048	2.66	8430410A17Rik	232210	RIKEN cdna 8430410A17 gene
3460296	2.64	Anxa2	12306	Annexin A2
460746	2.55	Dnmt3l	54427	DNA methyltransferase 3-like transcript variant 1
6200719	2.51	Acas2l	68738	Acyl-coa synthetase short-chain family member 1
5340731	2.50	Tcfcp2l3	252973	Grainyhead-like 2 (Drosophila)